

Serveur Académique Lausannois SERVAL serval.unil.ch

Author Manuscript

Faculty of Biology and Medicine Publication

This paper has been peer-reviewed but does not include the final publisher proof-corrections or journal pagination.

Published in final edited form as:

Title: A critical role of autophagy in antileukemia/lymphoma effects of APO866, an inhibitor of NAD biosynthesis.

Authors: Ginet V, Puyal J, Rummel C, Aubry D, Breton C, Cloux AJ, Majjigapu SR, Sordat B, Vogel P, Bruzzone S, Nencioni A, Duchosal MA, Nahimana A

Journal: Autophagy

Year: 2014 Apr

Volume: 10

Issue: 4

Pages: 603-17

DOI: 10.4161/auto.27722

In the absence of a copyright statement, users should assume that standard copyright protection applies, unless the article contains an explicit statement to the contrary. In case of doubt, contact the journal publisher to verify the copyright status of an article.

A critical role of autophagy in anti-leukemia/lymphoma effects of APO866, an inhibitor of NAD biosynthesis

Vanessa Ginet ^{1†}, Julien Puyal ^{1†}, Coralie Rummel ¹, Dominique Aubry ², Caroline Breton ², Anne-Julie Cloux ², Majjigapu S Red ³, Bernard Sordat ³, Pierre Vogel ³, Michel A. Duchosal ^{2‡} and Aimable Nahimana ^{2‡*}

¹Department of Fundamental Neurosciences Faculty of Biology and Medicine University of Lausanne Rue du Bugnon 9, CH-1005 Lausanne; Switzerland; ² Service and Central Laboratory of Hematology, University Hospital of Lausanne, Rue du Bugnon 46, 1011-CHUV Lausanne, Switzerland; ³Laboratory of Glycochemistry and Asymmetric Synthesis, Swiss Federal Institute of Technology (EPFL), Batochime, CH-1015 Lausanne, Switzerland

Running Title:

Key words: NAD, ATG, catalase, ROS, autophagy, APO866, lymphoma, leukemia, therapy

Corresponding Author:

Aimable Nahimana, PhD

Service of Hematology,

University Hospital of Lausanne (CHUV),

46, rue du Bugnon,

1011 Lausanne, Switzerland;

Telephone: +41-21-314-42-58; Fax: +41-21-314-41-80

e-mail: aimable.nahimana@chuv.ch

Text word count: 5071

Abstract word count: 177

Figure count: 9

Reference count: 43

†, ‡: These authors contributed equally and should be considered as co-first authors (†) and co-last authors (‡)

Abstract

APO866 is an inhibitor of NAD biosynthesis which exhibits potent antitumor properties in various malignancies. Recently, it has been shown that APO866 induces apoptotic and autophagy mediated cell death in human hematological cancer cells. However, the involvement of autophagy in APO866-induced cell death remains unclear. Here, we report studies on the molecular mechanisms underlying APO866-induced cell death with emphasis on autophagy. Treatment of hematological malignant cells with APO866 increases caspase activation as revealed by cleavage of caspase-3 and also enhances autophagic activities which are evidenced by an increase in autophagosome formation (LC3-II expression and LC3 punctate labeling). APO866-mediated autophagy selectively depletes catalase, a reactive oxygen species (ROS) scavenger, leading to ROS production and cell death. Inhibition of autophagy with lentivirally mediated transduction of shRNAs targeting the autophagic proteins ATG5, ATG7 and Beclin1 (ATG6) clearly abrogates APO866-induced cell death in hematopoietic malignant cells. Altogether, our results provide direct evidence that autophagy is essential for the cytotoxicity-mediated by APO866 on human leukemia cells, and open new way to enhancing the antitumor activities of APO866 by modulation of autophagic machinery.

Introduction

Inhibition of tumor growth by manipulating the cellular energy stores through nicotinamide and adenosine triphosphate (ATP) was theorized to be important mediators of the apoptotic biochemical cascade [1]. In this respect, several recent studies [2-5] reported the antitumor activities of a novel agent, APO866, that inhibits specifically nicotinamide phosphoribosyltransferase (NAMPT), a rate-limiting enzyme in the mammalian salvaging pathway for the synthesis of nicotinamide adenine dinucleotide (NAD) [6, 7]. NAD plays a crucial role as a cofactor/substrate in numerous biochemical and biological processes, including those catalyzed by poly(ADP-ribose) polymerase 1 (PARP1), sirtuins, and ADP-ribosyl cyclase [1-6]. NAMPT activity is essential for replenishing cellular NAD levels in mammalian cells, and the demand for NAD is tremendously increased in cancer cells compared with normal cells mainly due to genomic instability and persistent PARP1-dependent DNA repair [8, 9]. Thus, NAMPT has been shown to be an attractive therapeutic target for the development of new anticancer agents. Mechanistic studies revealed that APO866-mediated cell death involves NAD and ATP depletion, the loss of mitochondria membrane potential, caspase activation and autophagy-associated cell death [2, 3, 10, 11]. However, direct evidences of implication of autophagy in APO866-induced cell death are scarce.

Macroautophagy (hereafter called autophagy) is a physiological and essential self-digestion process for degradation of long-lived proteins and organelles and recycling of intracellular components [13]. During autophagy portions of cytosol containing the cellular material that need to be degraded are engulfed in multi-membrane vesicles termed autophagosomes. The mature autophagosomes fuses then with a lysosome, which contains the acidic hydrolases necessary for autophagic degradation creating a large compartment named autolysosomes

[12]. Autophagic degradation is important for basic homeostasis and for generation of amino acids and fatty acids used during protein synthesis and energy production. Autophagy is then often involved in cell survival when activated under starvation conditions [12-15]. However in other stress conditions enhanced autophagy could be implicated in promoting cell death as a mediator of apoptosis or necrosis or as an independent mechanism of death termed autophagic –associated cell death or programmed cell death type II (PCD II) [13]. To provide evidence of a pro-death role of autophagy, the common strategy has been to show that its inhibition protects or at least delays the cell death [14]. Several recent studies, have shown that certain forms of cell death are prevented in either the presence of pharmacological autophagy inhibitors or reduced autophagy related genes (ATG) expression, a group of autophagy regulatory genes conserved from yeast to humans [15], indicating that autophagy participates directly in the death process. Billington et al [10] and Cea et al, 2012 [16] reported that NAD synthesis inhibition induced autophagy in neuroblastoma and multiple myeloma cells, respectively. In addition, we previously showed that APO866-induced cell death in hematological malignant cells was attenuated in presence of pharmacological autophagy inhibitors [3]. These findings suggest that autophagy might be involved in APO866-induced cell death. However due to the incomplete specificity of these inhibitors definitive conclusion could not be made. To clarify the relationship between autophagy and APO866-induced cell death and to identify molecular mechanisms by which autophagy can be involved in leukemia cells death, we used in the present study specific inhibition of autophagy by lentiviral mediated transduction of shRNAs targeting three important Atg proteins: *Atg7*, *Atg5* and *Beclin1*. We now provide clear evidence that treatment of human leukemia/lymphoma cells with APO866 increases a Beclin1-independent autophagy involved in catalase degradation, one of the main cellular antioxidants. Consequent depletion of catalase results in increased ROS production and cell death. Inhibition of autophagy by

downregulation of *Atg5* and *Atg7* or extracellular addition of catalase abrogates APO866-induced cell death.

Materials and Methods

Reagents and antibodies

Clinical grade APO866 and Fas agonist (MegaFasL) were provided by TopoTarget (Lausanne, Switzerland). CaspGlow rhodamine active caspase-3, -8, and -9 staining kit was purchased from BioVision Inc (Milpitas, CA). The 5,5',6,6'-tetrachloro-1,1',3,3'-tetraethylbenzimidazolyl-carbocyanine iodide (JC-1) was purchased from Calbiochem (San Diego, CA). 2',7'-Dichlorofluorescein diacetate (DCFH-DA), chloroquine, and catalase were purchased from Sigma-Aldrich (St Louis, MO). Dihydroethidium and MitoSOX Red mitochondrial superoxide indicator were obtained from Life Technologies Europe BV (Paisley, United Kingdom); Annexin V-fluorescein isothiocyanate (FITC) and 7-aminoactinomycin D (7AAD) were purchased from Becton Dickinson Biosciences Pharmingen (San Diego, CA).

Cell lines and culture conditions

Seven different hematological cancer cell lines were herein evaluated. Cell lines were purchased from DSMZ (German Collection of Microorganisms and Cell Cultures, Braunschweig, Germany) or ATCC (Manassas, VA) and include: Jurkat and Molt-4 (T-acute lymphoblastic leukemia [T-ALL]); ML-2, MV4-11, and NOMO-1 (acute myeloid leukemia [AML]); Ramos (Burkitt' lymphoma [BL]); and RPMI8226 (Multiple myeloma).

Primary cells from 6 consenting patients were also analyzed. Study protocols were approved by the ethics committee at the University of Lausanne, and informed consent was obtained in accordance with the Declaration of Helsinki. Primary cells were collected from peripheral blood (purity > 90%) from patients with AML (n =1); and B-chronic lymphocytic leukemia (n=5, CLL).

All cells were cultured in RPMI (Gibco, Paisley, United Kingdom) supplemented with 10% heat inactivated fetal calf serum (FCS; Gibco) and 1% penicillin/streptomycin at 37°C (Bioconcept, Allschwil, Switzerland) in a humidified atmosphere of 95% air and 5% CO₂.

Flow cytometer analyses

Various cellular effects induced by APO866 on hematopoietic malignant cells were evaluated using a Beckman Coulter Cytomics FC500 flow cytometer and included following functional cell parameters: cell death, reactive oxygen species production, mitochondrial membrane potential, and caspase activation status.

Cell death analysis

APO866-induced cell death was determined using annexin-V and 7-aminoactinomycin D (7-AAD) stainings as described by the manufacturer and analyzed using a flow cytometer. Dead cells were identified as annexin V⁺ and/or 7AAD⁺.

Assessment of mitochondrial membrane potential

Mitochondrial membrane potential (MMP) was determined using a flow cytometer after cell staining with either JC-1 or TMRE. JC-1 and TMRE are cell permeants, fluorescent dyes that readily accumulates in active mitochondria due to their relative negative charge. JC-1 accumulates in the mitochondria, showing green fluorescence at a low mitochondrial membrane potential (MMP) and forming red fluorescent J-aggregates at higher membrane potential. Drop-in mitochondrial membrane potential is indicated by a decrease in the ratio of the red signal to the green signal. TMRE is a red-orange dye that readily accumulates in active mitochondria. Depolarized or inactive mitochondria have decreased membrane potential and fail to sequester TMRE. Briefly, cells were cultured in the presence or absence

of APO866 for 24 to 96 hours. Cells were centrifuged, resuspended in phosphate-buffered saline (PBS) containing 5 μ M JC-1 or 50 nM TMRE, and were then incubated at 37°C for 15 minutes in the dark. The cells were washed twice with pre-warmed PBS, and immediately analyzed using flow cytometry.

Detection of cellular and mitochondrial reactive oxygen species (ROS)

Intracellular levels of cytosolic and mitochondrial superoxide as well as hydrogen peroxide production were determined in APO866- and control- treated hematological malignant cells by flow cytometer using live-cell permeant specific fluorogenic probes, dihydroethidium (DHE), MitoSox, and DCFH-DA, respectively. DHE is oxidized to red fluorescent ethidium by cytosolic superoxide and MitoSox is selectively targeted to mitochondria, once in the mitochondria, it is oxidized by superoxide and exhibits red fluorescence. Whilst, DCFH-DA is cleaved by esterase to yield DCFH, a polar non-fluorescent product, but in presence of hydrogen peroxide the latter is oxidized to green fluorescent product, dichlorofluorescent (DCF). For cell staining, cells were centrifuged and the pellets were resuspended in PBS with a final concentration of 5 μ M for each probe. The mixture was incubated in dark at 37°C for 15 min. Then, the cell suspension was analyzed using a flow cytometer within 20 min.

Lentiviral vectors and virus production

Recombinant lentiviruses delivering anti-ATG shRNAs specific for human genes from TRC (the RNAi consortium) library in pLKO lentiviral vectors were used as follows: TRCN0000099431 for ATG5 (GenBankTM NM_004849), TRCN0000033552 for Beclin1 (GenBankTM NM_003766), and TRCN0000007584 for ATG7 (GenBankTM NM_006395) (Openbiosystems). Self-inactivating lentiviral vectors were produced by cotransfecting 293T cells with the lentivirus expression plasmid and packaging plasmids using the calcium

phosphate method. Infectious lentiviruses were harvested at 48h posttransfection, the supernatant was collected, filtered, concentrated by ultracentrifugation, re-suspended in 1% bovine serum albumin in PBS and then stored at -80°C until use as described previously (Perrin et al., 2007). Viral particle content was assayed for the p24 core antigen by using the p24 antigen enzyme-linked immunosorbent assay (RETROtek, Gentaur, Paris, France) according to the manufacturer's instructions.

Infection and generation of stable knockdown cell lines

To establish Jurkat or Ramos cell lines stably expressing a specific shRNA against ATGs, 6×10^6 Jurkat or Ramos cells were seeded in T25 cell culture flask and transduced with 50 ng of p24/ml culture medium for each vector. In parallel, Jurkat or Ramos cells were transduced with a lentiviral vector encoding a scramble shRNA (shRNA_{sc}) as an infection control. After 48 h, the transduced cells were selected by adding 10µg/ml Puromycin (Invitrogen) for three days.

Immunoblotting

Protein samples were harvested in lysis buffer containing 20 mmol/L HEPES, pH 7.4, 10 mmol/L NaCl, 3 mmol/L MgCl₂, 2.5 mmol/L EGTA, 0.1 mmol/L dithiothreitol, 50 mmol/L NaF, 1 mmol/L Na₃VO₄ or for LC3 expression analysis in a Tris-HCl buffer, pH 7.4, containing 150 mM NaCl, 5 mM EDTA, 1% triton X-100, 2mM sodium orthovanadate, 0.5mM phenylmethylsulphonyl fluoride, 0.05% aprotinin (w/v), and 1mM dithiotreitol. A protease inhibitor cocktail (Roche, 11873580001) was added. Lysates were sonicated and protein concentration was determined using a Bradford assay. Proteins (25–40 µg) were separated by SDS-PAGE on a 8, 10 or 14% polyacrylamide gel, and analyzed by immunoblotting. The following primary antibodies were used for protein immunodetection:

anti-APG7 (sc-33211, 1/1,000) rabbit polyclonal, anti-Beclin 1 (sc-11427, 1/1,000) and anti- α -actine (MAB1501, 1/1,000) mouse monoclonal antibodies from Millipore, anti-Beclin1 (sc-11427, 1/1000) from Santa Cruz Biotechnology; anti-LC3 (NB100-2220, 1/1,000) rabbit polyclonal antibody from Novus Biologicals; anti-catalase (#AF3398, 1/2000) goat polyclonal antibody from R&D systems, anti-active caspase-3 (#9661, 1/1,000) rabbit polyclonal antibodies from Cell Signaling Technology; anti p62/SQSTM1 (P0067, 1/1,000) rabbit polyclonal antibody from Sigma-Aldrich and anti-fodrin (#FG6090, 1/3,000) mouse monoclonal antibody from Biomol (Enzo Life Sciences). After incubation with primary antibody, the following secondary antibodies were applied: polyclonal goat anti-mouse or goat anti-rabbit IgG conjugated with IRDye 680 (LI-COR, B70920-02) or IRDye 800 (LI-COR, 926-32210). Protein bands were visualized using the Odyssey Infrared Imaging System (LI-COR). Odyssey v1.2 software (LI-COR) was used for densitometric analysis. OD values were normalized according to Ponceau staining as loading control and expressed as a percentage of values obtained for control non-treated cells (non-infected or infected with control vector transducing the scramble shRNA) (100%).

Immunocytochemistry and quantification of LC3-positive dots

Jurkat cells cultured in 6 wells plate were centrifuged, fixed with 4% paraformaldehyde in PBS (pH 7.4) for 20 min on ice and then plated on poly-L-lysine coated glass slides. Jurkat cells were first incubated for blocking and permeabilization in PBS with 10% donkey serum and 0.1% Triton X-100 for 30min. Then, cells were incubated with the anti-LC3 rabbit polyclonal antibody (Abcam, ab48394, 1/100) diluted in 1.5% of donkey serum in PBS overnight at 4°C. Alexa Fluor 488 donkey-anti-rabbit (Invitrogen, A21206) or Alexa Fluor 594 donkey-anti-rabbit (Invitrogen) secondary antibodies, diluted in PBS with 1% of donkey serum (1/200), were applied for 2 h at room temperature. After several washes in PBS,

Hoechst staining was done to reveal cell nuclei and slides were mounted with FluoroSave (Calbiochem, 345-789-20). Confocal images of immunocytochemistry against LC3 were acquired using a Zeiss LSM 710 confocal laser scanning microscope and images were then processed by with Adobe Photoshop 5.0. LC3-positive dots were analyzed using ImageJ software and expressed as a number of LC3-positive dots per cell per μm^2 .

Quantitative Real-Time RT-PCR

Total RNA was extracted using RNeasy Mini kit (Qiagen). Eluted RNA were analyzed (quantity and quality) using Agilent RNA 6000 Nano kit (Agilent Technologies). RNA was reverse transcribed to cDNA with the High Capacity cDNA Reverse Transcription kit (Applied Biosystem). Then, real-time quantitative PCR was performed with the MyiQ Single Color real-Time PCR detection system using iQ SyBR Green Supermix (Biorad) as described by Berta et al. 2008. The following primers were used for human Atg5: forward 5'-CCTTGGAACATCACAGTACAT-3', reverse 5'-CATCTTCAGGATCAATAGCAG-3'; human GAPDH: forward 5'-CCCCCAATGTATCCGTTGTG-3', reverse 5'-TAGCCCAGGATGCCCTTTAGT-3'.

Statistical Analysis

All assays were performed in triplicate and expressed as the mean and standard deviation (SD). All pairwise comparisons were analyzed by Tukey-Kramer Multiple comparisons Test or by one-way ANOVA followed by Student's t-test (2-tailed, 2-sample and unequal variance). GraphPad Prism version 6.00 (GraphPad Software, San Diego, CA) was used for statistical analysis. P values < .05 were considered statistically significant.

Results

APO866 enhances autophagy in hematological malignant cells

It is well known that APO866 triggers cell death in different types of malignant cells through NAD and ATP depletion. Several studies suggested various modes of cell death mechanisms induced by APO866, including apoptotic [2] [17-19] and autophagic [10, 16, 20] pathways. Although, the role of autophagy in cell death is under debate, evidences of autophagy-mediated cell death in treated-cancer cells are now being revealed [21-24]. A recently published study, clearly showed that APO866 exerts its anti-tumor activities in multiple myeloma cells, not through apoptosis, but rather induction of autophagy-associated cell death via transcriptional-dependent (transcription factor EB, TFEB) and –independent (PI3K-mTORC1) pathways [16, 25]. Multiple myeloma is a blood cancer characterized by the proliferation of plasma cells in the bone marrow. However, most of prior reports suggested that APO866 triggered apoptosis in various malignant cells [2, 17, 19, 26]. The contribution of apoptosis and autophagy in APO866-induced cell death seems to be cell dependent. We then examined whether APO866-induced cell death in leukemia/lymphoma cells is dependent on autophagic or apoptotic pathway. To provide evidence for autophagy induction in APO866-treated hematopoietic malignant cells, Jurkat cells were treated with or without APO866 and autophagic activity was determined by measuring (i) conversion of the cytoplasmic form of LC3 (LC3-I, 18KDa) to the preautophagosomal and autophagosomal membrane-bounded form of LC3 (LC3-II, 16KDa) by western blot, (ii) formation of LC3-positive vesicles by LC3 immunolabelling using confocal microscopy and (iii) degradation of protein p62, a protein selectively degraded by autophagy [27-29]. In a first time, APO866 induced a decrease in LC3-II level 24h after drug application. However this reduction was

followed by a significant increase in LC3-II suggesting a transitory activation of autophagy around 48h (Fig. 1A). This result was confirmed by the increase in LC3-positive dots in Jurkat cells treated with APO866 for 48h compared to control conditions, indicating an increase in autophagosome formation after APO866 treatment (Fig. 1B). To clarify whether increased autophagosome presence was due to enhanced autophagy flux or to reduced degradation of autophagosomes by defective lysosomal activity in APO866-treated Jurkat cells, we examined: (i) the expression level of p62 and (ii) monitored LC3-II conversion in presence of an inhibitor of autophagosome-lysosome fusion, chloroquine (CQ). Western blot analyses showed a decrease in p62 expression levels (Fig. 1C) and CQ treatment markedly increased LC3-II expression levels in APO866 treated-cells (Fig. 1D). These results demonstrate an increase of autophagic flux in Jurkat cells (enhanced autophagosome formation and active lysosomal degradation). Collectively, these findings support induction of autophagy in hematopoietic malignant cells after treatment with APO866.

APO866 induces caspase-dependent apoptosis in hematological malignant cells

This observation led us to examine whether apoptosis is also involved in the anti-leukemia effects of APO866. To this end, a time course analysis of caspase activation, a hallmark of apoptosis was evaluated in APO866-treated Jurkat cells. The caspases, a family of cysteine proteases, are subdivided into two groups: (a) initiator caspases, such caspase-8 and -9 [30], and (b) executioner caspases, such as caspase-3, -6, and -7 [31]. Western blot assay showed a steady increase of cleaved caspase-3 triggered by APO866 treatment in time dependent manner, and reaching a maximum at 72h (Fig. 2A). This observation suggests the involvement of caspase-dependent apoptotic pathway in anti-leukemic effects of APO866. To validate this finding, we then assessed activation of various caspases including caspase-8, -9,

and -3, on Jurkat cells treated for 72h with 10nM APO688 using the specific CaspGLOW™ Red Active for each caspase and flow cytometry. The caspGLOW assays offers a convenient way for measuring activated caspases in living cells. The assay uses a specific inhibitor for each caspase conjugated to sulfo-rhodamine as fluorescent marker which is cell permeable, non-toxic and irreversibly binds in specific manner to activated caspase in apoptotic cells. The red fluorescence label allows for direct detection of activated caspase in apoptotic cells by flow cytometry. APO866 treatment tremendously increases caspase-8, -9, and -3 activities in Jurkat cells (Fig. 2B), indicating that caspase-dependent apoptosis is involved in anti-leukemia effects of APO866. To confirm whether the apoptosis induced by APO866 is not only restricted to Jurkat cells, hematopoietic cancer cells from 2 additional cell lines (ML2: acute myeloid leukemia M4; Ramos: Burkitt lymphoma) from different hematological malignancies were incubated with APO866 for 72 hours, and caspase activities detected as mentioned above. APO866 also elicited a high level of caspases activity in Ramos and ML2 cells (Supplementary Fig. S1), confirming the involvement of apoptosis in the antitumor activities exerted by APO866 in various hematopoietic tumor cells. Unlike results reported for multiple myeloma cells [16], these results indicate that APO866 can induce both autophagy and apoptosis in human leukemia/lymphoma cells.

Beclin1-independent autophagy is required for anti-leukemia/lymphoma effects of APO866

Induction of autophagy has been proven to be either a survival-promoting [32] or a pro-death pathway depending on the stress conditions even if its exact implication in cell death remains controversial [13, 33]. In our previous study delineating mechanisms involved in APO866-induced cell death in hematological malignancies, the implication of autophagy in this process was not clearly demonstrated but only suggested by the protective effect of autophagy pharmacological inhibitors [3]. In fact, we showed that PI3K inhibitors (3-methyladenine,

wortmanin, and LY294002) were capable of attenuating APO866-induced cell death in hematological malignancies, suggesting a contribution of autophagy in mediating cell death. However, PI3K inhibitors may affect both class I and III PI3K, which are implicated in various biological pathways. To provide strong evidences of specific implication of autophagy in APO866-induced cell death, autophagy was inhibited using lentiviral mediated transduction of shRNAs targeting *Atg5*, *Atg7* and *Beclin1* whose expressions are required to form autophagosomes. To provide evidences that autophagy-mediated cell death was not cell-type dependent, the cytotoxic effect of APO866 was investigated in two selected (Jurkat and Ramos) lines from different hematological malignancies. If autophagy is involved in APO866-induced cell death, silencing *Atg5*, *Atg7* or *beclin1* will provide protection against APO866 treatment. Decreased *beclin1*, *Atg5*, and *Atg7* expressions in transduced-Jurkat (Fig. 3A-C) and Ramos (Supplementary Fig. 2A-C) cells were confirmed by either Western blot or RT-PCR. In addition, lentiviral vectors delivering shRNA against *beclin1*, *Atg5* and *Atg7* decreased LC3-II accumulation produced after 6h in presence of CQ in Jurkat and Ramos cells (Fig. 3D and Supplementary Fig. 2D), validating the KD effect of each *Atg* by showing that autophagosome formation is reduced in these transduced malignant cells. Importantly, downregulation of ATG5 and ATG7, but not Beclin1 expression abrogated APO866-induced cell death in Jurkat and Ramos cells (Fig. 5A and Supplementary Fig. 3A) and this protection could still be observed 10 days after drug treatment (Fig. 5B and Supplementary Fig. 3B). These results clearly indicate that autophagy is a key player in APO866-induced cell death in Leukemia/lymphoma cells.

Since caspase activation was detected in APO866-treated leukemia/lymphoma cells, we next examined whether APO866-induced cell death was also caspase-dependent. To this end, Jurkat, Ramos, and ML2 were treated with APO866 at different time points, and in presence or absence of a broad caspase inhibitor, z-VAD. Our results revealed that caspase inhibition

delayed but not prevented APO866-induced cell death (Fig. 6A and Supplementary Fig. 4), which suggests that caspases inhibition is not effective to prevent APO866-induced cytotoxicity. Moreover when caspase-3 activation was assessed by Western blot in Jurkat cells that are knockdown for *Atg5* and *Atg7*. Cleavage of caspase-3 was fully prevented 72h after APO866 treatment compared to control vector infected and shRNA Beclin1 transduced cells (Fig. 6B and Supplementary Fig. 4B). This result suggests that autophagy induction acts upstream of caspase-3 and may contribute to its activation.

Taken together, these results strongly suggest that APO866 induces cell death (i) highly dependent on autophagy, (ii) with activation of caspases which (iii) is regulated by autophagy.

APO866 induces reactive oxygen species generation through autophagy-dependent catalase degradation

We and others demonstrated that APO866 is a highly potent NAD depleting agents in various malignant cells [2, 3, 11, 16, 17, 20]. NAD(P)H/NAD(P)⁺ cell contents play a crucial role in numerous redox reactions. Cellular redox status is one of the main mechanisms involved in control and regulation of cell death pathways, including apoptotic, autophagic and necrotic processes. Depleting NAD is expecting to induce perturbation of NAD(P)H/NAD(P)⁺ ratio which will result in production of high levels of reactive oxygen species (ROS) that would lead to cell death. We then hypothesized that NAD depletion induced by APO866 in hematological malignant cells would result in increased ROS production that would lead to cell damage and finally to cell death. To test this issue, cytosolic and mitochondrial superoxide productions as well as intracellular hydrogen peroxide were monitored in various hematological malignant cells treated with APO866 using DHE and Mitosox as well as DCFH-DA probe respectively. As expected, APO866 caused an increase level of both

cytosolic and mitochondrial ROS in all treated hematopoietic malignant cells (Fig. 7A and Supplementary Fig. 5A). As excessive ROS generation leads to mitochondrial damages, these findings are consistent with our previous study that reported the mitochondria depolarization in APO866-treated leukemia/lymphoma cells [3]. ROS accumulation may be caused by either an increase in ROS production or decreased ROS degradation. To explain the burst of ROS production in APO866-treated leukemia/lymphoma cells, we then investigated whether catalase, one of the key enzymatic ROS scavengers, was degraded in hematopoietic malignant cells from different hematological malignancies in presence of APO866. Western blot analysis demonstrated a decrease in catalase expression in all analyzed malignant cell lines in time-dependent manner (Fig. 7B and Supplementary Fig. 5B) suggesting a involvement of catalase degradation in ROS production.

Autophagy acts upstream of ROS generation and mitochondrial depolarization in APO866-treated malignant cells

It has been shown that autophagy can be in some cases regulated by ROS (Chen et al., 2009, Scherz-Shouval et al., 2007; Szumiel, 2010) and in other cases be involved in ROS production (Kubota et al, 2010). To determine whether ROS accumulation in APO866-treated hematopoietic tumor cells is upstream or downstream of autophagy induction, we investigated the effect of ATG5 and ATG7 downregulation on ROS production. If ROS is acting upstream of autophagy induction, inhibition of autophagy with genetic approaches will have no effect on ROS production. Otherwise, autophagy inhibition will decrease or prevent ROS. To determine the role played by autophagy in APO866-induced ROS generation, shRNA transduced Jurkat and Ramos cells were exposed to APO866 for 72h and intracellular ROS production was measured using Mitosox, DCFH-DA and flow cytometer. Our data showed that downregulation of ATG5 and ATG7 strongly reduced the APO866-induced ROS

production (Fig. 8A-B and Supplementary Fig. 6A-B) compared to control vector and shRNA Beclin1 transduced or wt cells (Fig. 7A). This argues for autophagy induction upstream of ROS production.

Autophagy degrades selectively catalase in APO866-treated malignant cells

It has been reported that catalase could be a selective substrate of autophagy in condition of autophagy-mediated cell death [34]. Catalase degradation in APO866-treated hematological malignant cells could be then a way for autophagy to regulate ROS production. To test this hypothesis, Jurkat cells downregulated for Beclin1, ATG5 and ATG7 were incubated with or without APO866 for 72 hours and expression level of catalase was determined by western blot assay. Inhibition of autophagy by transduction of shRNA Atg5 and Atg7 totally abrogated catalase depletion on the contrary of transduction of shRNA Beclin1 and control vector (Fig. 8C and Supplementary Fig. 6C). Consequently, inhibition of *beclin1*-independent autophagy also prevented the mitochondrial depolarization induced by APO866 treatment (Fig. 8D Supplementary Fig. 6D). Altogether, these data strongly suggest that APO866-induced autophagy is involved in catalase degradation and subsequent excessive ROS production which leads to loss of mitochondrial membrane potential and ultimately to cell death.

Exogenous addition of catalase abrogates the anti-leukemic/lymphoma effects of APO866

According to our data catalase appears to play a pivotal role in APO86-induced cell death in hematopoietic tumor cells. To provide evidence of involvement of catalase degradation in APO866-induced cell death, cells from lines and primary cells from patients diagnosed with various hematological malignancies were treated with or without APO866 in presence or absence of exogenous addition of catalase and cell death was monitored using annexin-V/7-

aminoactinomycin-D (7-AAD) and flow cytometer. As expected, extracellular addition of catalase, completely blocked APO866-induced cell death in all analyzed tumor cells, independently of hematological malignancies (Fig. 9), highlighting its essential role in APO866-antitumor activities. Importantly, the protective effects of catalase were observed over a week after APO866 treatment (Fig. 9B). This finding confirms that catalase play a major role in APO866-induced cell death.

Discussion

In the present study, we show that treatment of leukemia/lymphoma cells with APO866 induces both autophagy and apoptosis, and that suppression of autophagy prevents APO866-induced caspase activation in hematopoietic malignant cells. This suggests a crosstalk between autophagy and apoptosis.

Apoptosis was revealed by observing increases in activation of caspase-8, -9, and -3 using flow cytometer and accumulation of cleaved caspase-3 fragment in APO866-treated malignant cells. Our data further reveals that pan-caspase inhibitor could not prevent, but only delay APO866-induced cell death, suggesting that both caspase-dependent and -independent cell death modes are involved. This confirms previous studies evidencing that apoptosis is a mechanism acting in APO866-induced cell death [2, 4, 17, 19], but tempers its strong association in hematological cancers studied here.

We confirm here the involvement of autophagy, and indeed found that it plays an essential role, in such death. Evidences of autophagy induction in leukemia/lymphoma cells treated with APO866 were provided by (i) by western blot assays showing an accumulation of LC3-II and degradation of p62; (ii) immunoblotting through increased formation of LC3 punctuas, and (iii) inhibition of autophagic markers in hematopoietic malignant cells knockdown in atg-5 and -7, but not beclin. These latter inhibitions completely block APO866-induced cell death in different hematopoietic malignant cells, which provide the proof of direct implication of this autophagy loop in APO866- induced in leukemia/lymphoma cell death. In the last decade, autophagy has been extensively studied (refs...). In most studies, autophagy is functioning as survival mechanism under stress conditions (refs...). Its role in cell death is not well established. In efforts to elucidate molecular mechanisms by which APO866 triggers autophagy-associated cell death in leukemia/lymphoma cells, our results demonstrate that APO866 treatment in various hematopoietic malignant cells increases autophagic activities

which results in catalase degradation. Thus, depletion of catalase led to ROS (cytosolic and mitochondrial superoxide as well as intracellular hydrogen peroxide) accumulation and finally to cell death. To delineate the importance of catalase depletion in APO866, we show that exogenous addition of catalase totally blocked the APO866 killing effects in various hematological malignant cells. These findings provide for the first time the crucial role of antioxidants (catalase) in autophagy-associated cell death in APO866-treated hematopoietic malignant. However, based on our results, we cannot rule out the implication of other antioxidant enzymes in this process. Indeed, there are other antioxidants playing the same role as catalase in cell detoxification, i.e., glutathione peroxidase (GPx), and peroxiredoxin III (PrxIII). All these enzymes convert H₂O₂ to H₂O (refs...). Additionally, extracellular addition of catalase has been reported to lower superoxide anion and by this way masking the effects of SOD depletion [35, 36]. Further experiments are warranted to explore the effects of APO866 treatment on all antioxidant enzymes in tumor cells.

Our findings are consistent with previous studies that showed the implication of autophagy in cell (including myeloma cell) death ([10, 16, 20]. refs...), extend it to leukemia/lymphoma cells, and reveal that autophagy is essential for observing APO866-induced caspase activation in hematopoietic malignant cells. Autophagy may control apoptosis in APO866-treated leukemia/lymphoma cells through ROS production. We provide evidences that APO866 triggers a tremendous increase of ROS production via antioxidant depletion. High level of ROS production is known to be deleterious for cell health, since it oxidizes proteins, lipids, and cell organelles, including mitochondria ending with cell death. This explains the depolarization of mitochondria observed in APO866-treated hematopoietic malignant cells. Furthermore, accumulation of ROS in mitochondria is known to impair ATP production, induce membrane permeabilization, and lead to apoptosis. Consequently, inhibition of autophagy will preserve the cellular antioxidant contents, which will block APO866-induced

ROS production, and thus avoiding apoptosis. Importantly, unlike previous studies published elsewhere, autophagy induced by APO866 treatment in leukemia/lymphoma is upstream of ROS production. Here, we did not address how APO866 initiates autophagy in leukemia/lymphoma cells; it could be through inhibition of mTORC1 and via TFEB pathways, as it was shown in multiple myeloma cells [25]. Question whether this issue is similar in leukemia/lymphoma cells needs to be clarified.

In conclusion, we demonstrate induction of autophagy and apoptosis upon APO866 treatment in leukemia/lymphoma cells. Apoptosis was induced by both caspase-dependent and -independent pathways and was under control of autophagy. Autophagy-associated cell death was likely induced in non-canonical pathways; i.e., through atg5/atg7-dependent pathways. These findings open new way of modulating autophagic machinery as approach of enhancing the antitumor activities of APO866. Efforts to unravel the molecular mechanisms underlying APO866-induced cytotoxicities in various tumor cells are expected to greatly improve our understanding of mechanisms that take part in control of APO866-induced cell death. This may provide a stepping stone towards future development of novel anticancer therapy approaches.

Acknowledgements

This work was supported by a grant from the Faculty of Biology and Medicine of the University of Lausanne and the Fondation Dr Henri Dubois-Ferrière Dinu Lipatti.

Author contribution statement

VGP, JP, designed, executed and analyzed experiments and wrote the paper. CR, DA, CB, AJC performed, and analyzed the data. MSR, BS, PV analyzed results and wrote the paper.

MAD designed and analyzed experiments, coordinated the project, and wrote the paper. A.N. designed, executed and analyzed experiments, coordinated the project, and wrote the paper.

Conflict of interest

The authors declare no competing financial interest

Reference

- [1] Martin DS, Schwartz GK. Chemotherapeutically induced DNA damage, ATP depletion, and the apoptotic biochemical cascade. *Oncology research*. 1997;9(1):1-5.
- [2] Hasmann M, Schemainda I. FK866, a highly specific noncompetitive inhibitor of nicotinamide phosphoribosyltransferase, represents a novel mechanism for induction of tumor cell apoptosis. *Cancer research*. 2003 Nov 1;63(21):7436-42.
- [3] Nahimana A, Attinger A, Aubry D, Greaney P, Ireson C, Thougard AV, et al. The NAD biosynthesis inhibitor APO866 has potent antitumor activity against hematologic malignancies. *Blood*. 2009 Apr 2;113(14):3276-86.
- [4] Zhang LY, Liu LY, Qie LL, Ling KN, Xu LH, Wang F, et al. Anti-proliferation effect of APO866 on C6 glioblastoma cells by inhibiting nicotinamide phosphoribosyltransferase. *European journal of pharmacology*. 2012 Jan 15;674(2-3):163-70.
- [5] Zoppoli G, Cea M, Soncini D, Fruscione F, Rudner J, Moran E, et al. Potent synergistic interaction between the Nampt inhibitor APO866 and the apoptosis activator TRAIL in human leukemia cells. *Experimental hematology*. 2010 Nov;38(11):979-88.
- [6] Berger F, Lau C, Dahlmann M, Ziegler M. Subcellular compartmentation and differential catalytic properties of the three human nicotinamide mononucleotide adenylyltransferase isoforms. *The Journal of biological chemistry*. 2005 Oct 28;280(43):36334-41.
- [7] Revollo JR, Grimm AA, Imai S. The regulation of nicotinamide adenine dinucleotide biosynthesis by Nampt/PBEF/visfatin in mammals. *Current opinion in gastroenterology*. 2007 Mar;23(2):164-70.
- [8] Hufton SE, Moerkerk PT, Brandwijk R, de Bruine AP, Arends JW, Hoogenboom HR. A profile of differentially expressed genes in primary colorectal cancer using suppression subtractive hybridization. *FEBS letters*. 1999 Dec 10;463(1-2):77-82.
- [9] Van Beijnum JR, Moerkerk PT, Gerbers AJ, De Bruine AP, Arends JW, Hoogenboom HR, et al. Target validation for genomics using peptide-specific phage antibodies: a study of five gene products overexpressed in colorectal cancer. *International journal of cancer Journal international du cancer*. 2002 Sep 10;101(2):118-27.
- [10] Billington RA, Genazzani AA, Travelli C, Condorelli F. NAD depletion by FK866 induces autophagy. *Autophagy*. 2008 Apr;4(3):385-7.
- [11] Bruzzone S, Fruscione F, Morando S, Ferrando T, Poggi A, Garuti A, et al. Catastrophic NAD⁺ depletion in activated T lymphocytes through Nampt inhibition reduces demyelination and disability in EAE. *PloS one*. 2009;4(11):e7897.
- [12] Klionsky DJ, Emr SD. Autophagy as a regulated pathway of cellular degradation. *Science*. 2000 Dec 1;290(5497):1717-21.
- [13] Clarke PG, Puyal J. Autophagic cell death exists. *Autophagy*. 2012 Jun;8(6):867-9.
- [14] Lenardo MJ, McPhee CK, Yu L. Autophagic cell death. *Methods in enzymology*. 2009;453:17-31.
- [15] Ohsumi Y. Molecular dissection of autophagy: two ubiquitin-like systems. *Nature reviews Molecular cell biology*. 2001 Mar;2(3):211-6.
- [16] Cea M, Cagnetta A, Fulciniti M, Tai YT, Hideshima T, Chauhan D, et al. Targeting NAD⁺ salvage pathway induces autophagy in multiple myeloma cells via mTORC1 and extracellular signal-regulated kinase (ERK1/2) inhibition. *Blood*. 2012 Oct 25;120(17):3519-29.
- [17] Thakur BK, Dittrich T, Chandra P, Becker A, Kuehnau W, Klusmann JH, et al. Involvement of p53 in the cytotoxic activity of the NAMPT inhibitor FK866 in myeloid leukemic cells. *International journal of cancer Journal international du cancer*. 2013 Feb 15;132(4):766-74.
- [18] Okumura S, Sasaki T, Minami Y, Ohsaki Y. Nicotinamide phosphoribosyltransferase: a potent therapeutic target in non-small cell lung cancer with epidermal growth factor receptor-gene

mutation. *Journal of thoracic oncology : official publication of the International Association for the Study of Lung Cancer*. 2012 Jan;7(1):49-56.

- [19] Muruganandham M, Alfieri AA, Matei C, Chen Y, Sukenick G, Schemainda I, et al. Metabolic signatures associated with a NAD synthesis inhibitor-induced tumor apoptosis identified by 1H-decoupled-31P magnetic resonance spectroscopy. *Clinical cancer research : an official journal of the American Association for Cancer Research*. 2005 May 1;11(9):3503-13.
- [20] Travelli C, Drago V, Maldi E, Kaludercic N, Galli U, Boldorini R, et al. Reciprocal potentiation of the antitumoral activities of FK866, an inhibitor of nicotinamide phosphoribosyltransferase, and etoposide or cisplatin in neuroblastoma cells. *The Journal of pharmacology and experimental therapeutics*. 2011 Sep;338(3):829-40.
- [21] Chen SY, Chiu LY, Maa MC, Wang JS, Chien CL, Lin WW. zVAD-induced autophagic cell death requires c-Src-dependent ERK and JNK activation and reactive oxygen species generation. *Autophagy*. 2011 Feb;7(2):217-28.
- [22] Seo G, Kim SK, Byun YJ, Oh E, Jeong SW, Chae GT, et al. Hydrogen peroxide induces Beclin 1-independent autophagic cell death by suppressing the mTOR pathway via promoting the ubiquitination and degradation of Rheb in GSH-depleted RAW 264.7 cells. *Free radical research*. 2011 Apr;45(4):389-99.
- [23] Shimizu S, Konishi A, Nishida Y, Mizuta T, Nishina H, Yamamoto A, et al. Involvement of JNK in the regulation of autophagic cell death. *Oncogene*. 2010 Apr 8;29(14):2070-82.
- [24] Grishchuk Y, Ginet V, Truttman AC, Clarke PG, Puyal J. Beclin 1-independent autophagy contributes to apoptosis in cortical neurons. *Autophagy*. 2011 Oct;7(10):1115-31.
- [25] Cea M, Cagnetta A, Patrone F, Nencioni A, Gobbi M, Anderson KC. Intracellular NAD (+) depletion induces autophagic death in multiple myeloma cells. *Autophagy*. 2012 Dec 5;9(3).
- [26] Thakur BK, Dittrich T, Chandra P, Becker A, Lippka Y, Selvakumar D, et al. Inhibition of NAMPT pathway by FK866 activates the function of p53 in HEK293T cells. *Biochemical and biophysical research communications*. 2012 Aug 3;424(3):371-7.
- [27] Bjorkoy G, Lamark T, Brech A, Outzen H, Perander M, Overvatn A, et al. p62/SQSTM1 forms protein aggregates degraded by autophagy and has a protective effect on huntingtin-induced cell death. *The Journal of cell biology*. 2005 Nov 21;171(4):603-14.
- [28] Pankiv S, Clausen TH, Lamark T, Brech A, Bruun JA, Outzen H, et al. p62/SQSTM1 binds directly to Atg8/LC3 to facilitate degradation of ubiquitinated protein aggregates by autophagy. *The Journal of biological chemistry*. 2007 Aug 17;282(33):24131-45.
- [29] Ichimura Y, Kumanomidou T, Sou YS, Mizushima T, Ezaki J, Ueno T, et al. Structural basis for sorting mechanism of p62 in selective autophagy. *The Journal of biological chemistry*. 2008 Aug 15;283(33):22847-57.
- [30] Wang ZB, Liu YQ, Cui YF. Pathways to caspase activation. *Cell biology international*. 2005 Jul;29(7):489-96.
- [31] Creagh EM, Conroy H, Martin SJ. Caspase-activation pathways in apoptosis and immunity. *Immunological reviews*. 2003 Jun;193:10-21.
- [32] Kuma A, Hatano M, Matsui M, Yamamoto A, Nakaya H, Yoshimori T, et al. The role of autophagy during the early neonatal starvation period. *Nature*. 2004 Dec 23;432(7020):1032-6.
- [33] Kroemer G, Levine B. Autophagic cell death: the story of a misnomer. *Nature reviews Molecular cell biology*. 2008 Dec;9(12):1004-10.
- [34] Yu L, Wan F, Dutta S, Welsh S, Liu Z, Freundt E, et al. Autophagic programmed cell death by selective catalase degradation. *Proceedings of the National Academy of Sciences of the United States of America*. 2006 Mar 28;103(13):4952-7.

Legends

Figure 1. APO866 induces autophagy in Jurkat cells. (A) Western blot analysis and corresponding quantification of LC3-II form in untreated control cells (ct) and treated Jurkat cells. Malignant cells were incubated with APO866 (10 nM) at different time points. The LC3-II protein was detected by western blot using a specific polyclonal antibody. Relative intensity of LC3-II was calculated by normalizing the LC3-II intensity to actin using ImageJ Version 1.46 analysis software. Data are mean \pm SD, $n \geq 7$. (B) Confocal images of Jurkat cells immunolabelled for LC3 (in red) and Hoechst-stained (nuclei) with quantification of the number of LC3-positive dots (autophagosomes) per cell per μm^2 demonstrate that exposure to APO866 for 48h. $n=40$. Bar = $10\mu\text{m}$. Fluorescence was recorded using a Nikon E800 epifluorescence microscope equipped with a Coolsnap CF color camera (Nikon; 40x magnification). Quantification of LC3-positive dots per cells per μm^2 . Data are mean \pm SD; $n= 40$ cells per conditions. Bar = $10\mu\text{m}$. (C) Western blot analysis and corresponding quantification of p62 protein in untreated control cells (ct) and treated Jurkat cells. Cells were cultured as mentioned in (A) and p62 detected using specific polyclonal antibody. Data are mean \pm SD, $n \geq 5$. (D) Western blot analysis and corresponding quantification of LC3-II form in untreated control cells (ct) and treated Jurkat cells in presence of chloroquine, a lysosomal inhibitor. Jurkat cells were pre-treated with 25 CQ μM for 1 hour before APO866 treatment for 72 hours. LC3-II was detected and quantified as mentioned above. Data are mean \pm SD, $n \geq 5$. ** $p < 0.01$; *** $p < 0.001$.

Figure 2. APO866 activates caspases in Jurkat cells. (A) Western blot and corresponding quantification of cleaved caspase-3 in untreated control cells (ct) or at different time points after APO866 (10nM) treatment. Jurkat cells were incubated with APO866 (10 nM) at different time points. The 19 and 17kDa fragments of caspase-3 (cleaved forms) were detected by western blot using a specific polyclonal antibody. Relative intensity of cleaved caspase-3 forms were similarly calculated as in Fig. 1A. Data are mean \pm SD; *** $p < 0.001$; $n \geq 5$. (B) Detection of fluorescent activated caspases. Jurkat cells were treated with 10 nM APO866 for 72 hours and activated forms of

caspase-3, -8, and -9 were detected using fluorescent probe specific for each caspase and flow cytometry. Data are representative of three independent experiments.

Figure 3. *Beclin1*, *Atg7* and *Atg5* are efficiently downregulated in Jurkat cells. Jurkat cells were transduced with either control scrambled or lentiviral constructs expressing shRNA targeting *Atg5*, *Atg7*, and *beclin1*. 48 hours after transduction, cell lysates or mRNA were subjected to Western blot analysis or RT-PCR to monitor BECLIN (A), ATG7 (B) protein or *Atg5* mRNA (C) expressions, respectively. (D) Western blot analysis and corresponding quantification of LC3-II form in untreated control Jurkat cells transduced with either control scrambled or lentiviral constructs expressing shRNA targeting *Atg5*, *Atg7*, and *beclin1*. Cells deficient in autophagy were cultured with CQ for 6 hours and LC3-II protein expressions were assessed by Western blot and quantified as mentioned above. . Data are mean \pm SD, n = 6. **p<0.01; ***p<0.001.

Figure 4. Downregulation of *Atg5* and *Atg7* prevent APO866-induced autophagy in Jurkat cells. Western blot analysis and corresponding quantification of p62 protein in untreated (ct) or APO866-treated Jurkat cells knocked down for *beclin 1*, *Atg5* and *Atg7*. Malignant cells were cultured in presence or absence of 10nM APO866 for 72 hours and cell lysates were subjected to Western blot analysis to assess p62 protein expression. Data are mean \pm SD, n \geq 6. *p<0.05, ***p<0.001.

Figure 5. Autophagy is required for APO866-induced cell death. Cell death induced by APO866 on wild type and autophagy deficient Jurkat cells. Cell death was assessed by flow cytometry using annexin-V and 7AAD stainings after 72 hours (A) and 240 hours (B) treatments. The percentage of early apoptotic cells (annexin V+7AAD-) are shown as white columns and that of late apoptotic cells (annexin V+7AAD+) are shown as solid black columns. Data are mean \pm SD, n \geq 3. ***p<0.001.

Figure 6. Autophagy contributes to APO866-induced caspase-3 activation in Jurkat cells. (A) Time course analysis of cell death induced by APO866 on Jurkat cells in

presence of pan-caspase inhibitor, zVAD-fmk Wild type Jurkat cells were exposed to 10 nM APO866 in presence of 100 μ M zVAD-fmk and cell death was monitored as mentioned in Fig. 5. Data are mean \pm SD, n=3. **p<0.01. **(B)** Western blot analyses and corresponding quantifications of cleaved caspase-3 in scrambled (sc) and autophagy deficient Jurkat cells. Cells were exposed to 10 nM APO866 and cleaved caspase-3 forms were detected and quantified as mentioned above. Data are mean \pm SD, n \geq 10. *p<0.05, **p<0.01; ***p<0.001.

Figure 7. APO866 induces ROS generation and catalase degradation in Jurkat cells.

(A) Detection of ROS production in Jurkat cells treated with APO866. Cells were incubated without or with 10 nM APO866 and cytosolic, mitochondrial superoxide and hydrogen peroxide were detected by flow cytometry using DHE, mitosox, and DCFDA fluorescent probe, respectively. Data are mean \pm SD, n=3; ***p<0.001. **(B)** Western blot analysis and corresponding quantifications of catalase expression in wild-type Jurkat cells. Cells were exposed to 10 nM APO866 and catalase expression was detected and quantified in time dependent manner as mentioned above. . Data are mean \pm SD, n \geq 9. *p<0.05, **p<0.01; ***p<0.001.

Figure 8. Autophagy is involved in APO866-induced ROS generation and catalase degradation in Jurkat cells.

Detection of ROS production in wild type and autophagy deficient Jurkat cells exposed to APO866. Cells were incubated without or with 10 nM APO866 and mitochondrial superoxide **(A)** and hydrogen peroxide **(B)** were detected as mentioned above. Data are derived from at least 3 independent experiments. **(C)** Western blot analysis and corresponding quantifications of catalase expression in wild type and autophagy deficient Jurkat cells exposed to APO866. Cells were exposed to 10 nM APO866 for 72 hours and catalase expression was detected and quantified as mentioned above. Data are mean \pm SD, n \geq 8. ***p<0.001. **(D)** Detection of Mitochondrial potential in wild type and autophagy deficient Jurkat cells exposed to APO866. Cells were incubated without or with 10 nM APO866 and the mitochondrial potential was measured

using JC-1 and flow cytometry staining red versus green fluorescence as described in “Methods.” Data are derived from at least 3 independent experiments. *** $p < 0.001$.

Figure 9. Extracellular addition of catalase prevents APO866-mediated cell death in various hematopoietic malignant cells. Cells were incubated with or without 500 (or 1000) U catalase in presence or absence of 10 nM APO866. Cell death was assessed 96 hours (A) and 168 hours (B) after drug exposure and as described above. Data are derived from at least 3 independent experiments.

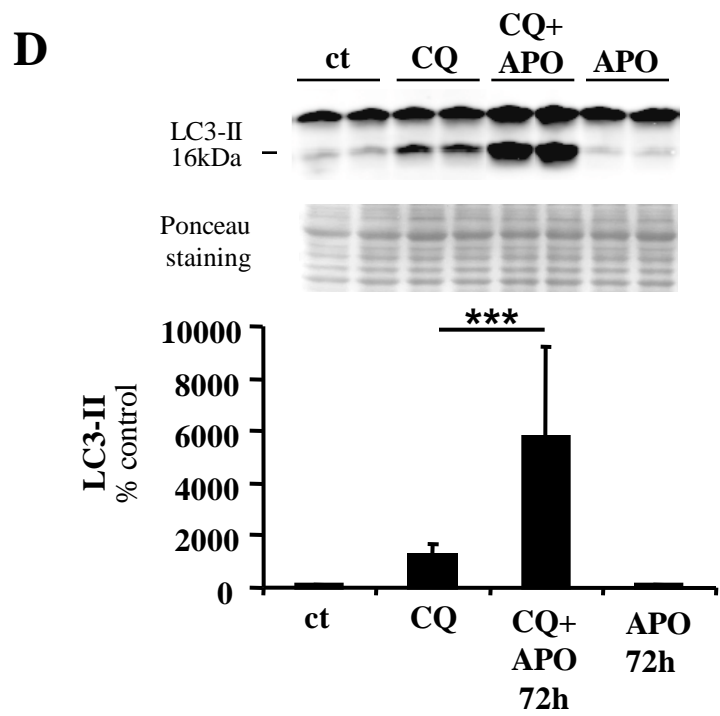
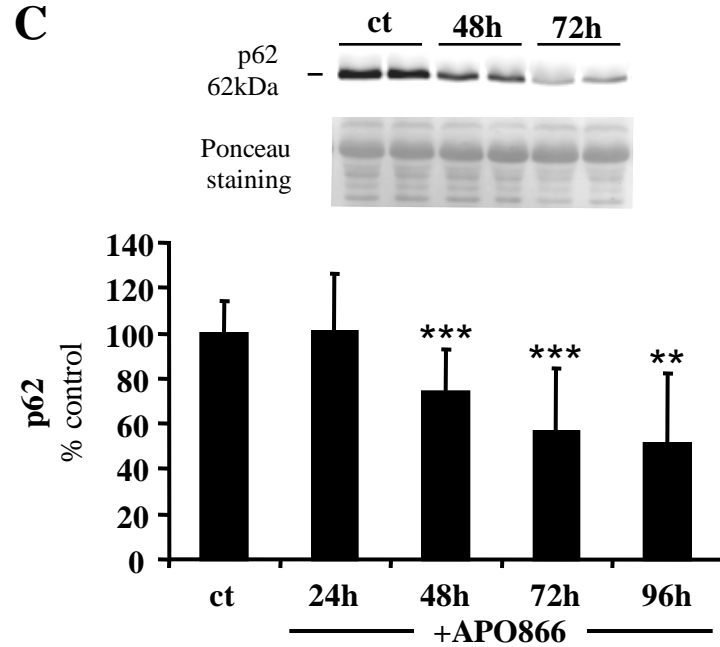
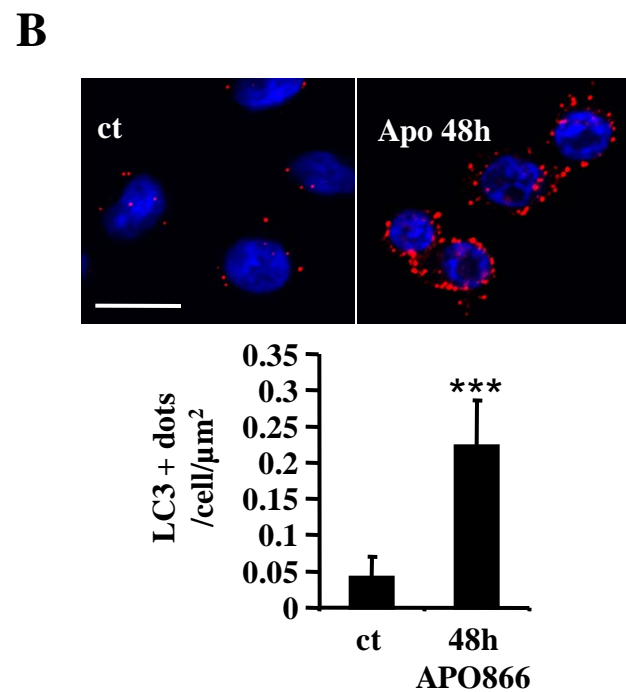
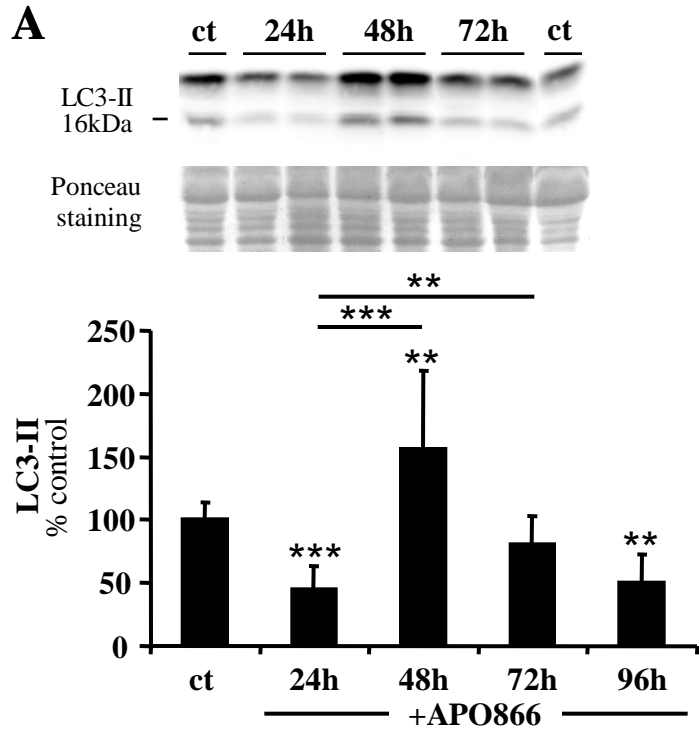
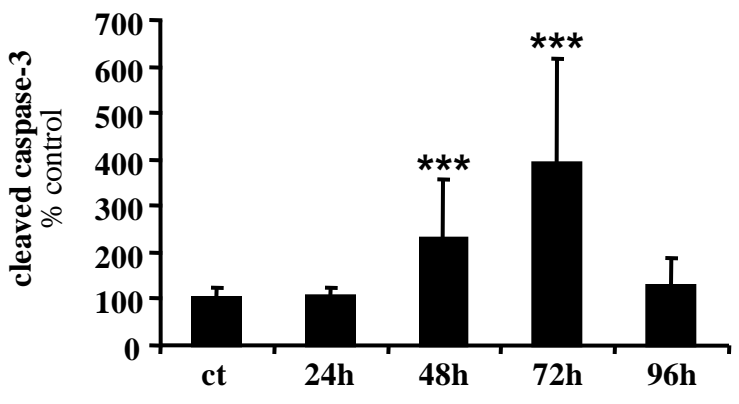
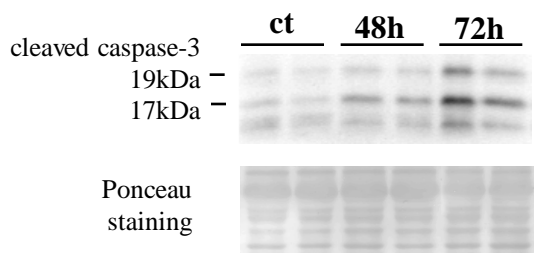
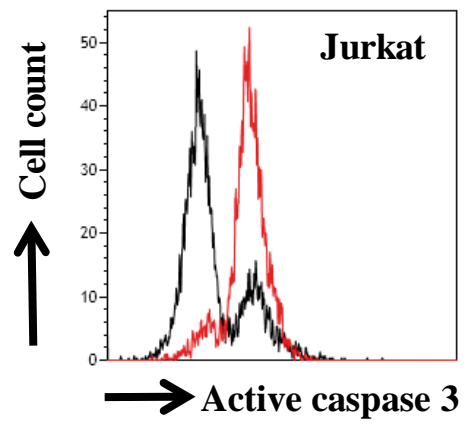


Fig. 2

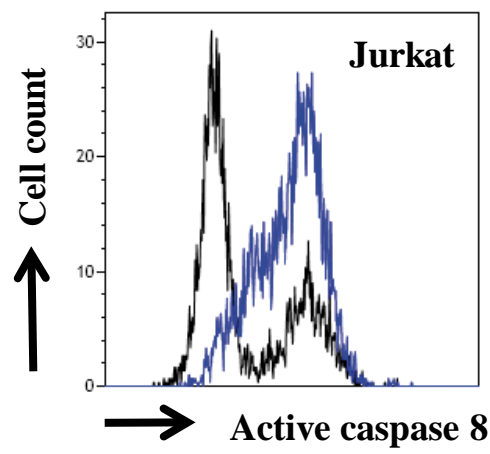
A



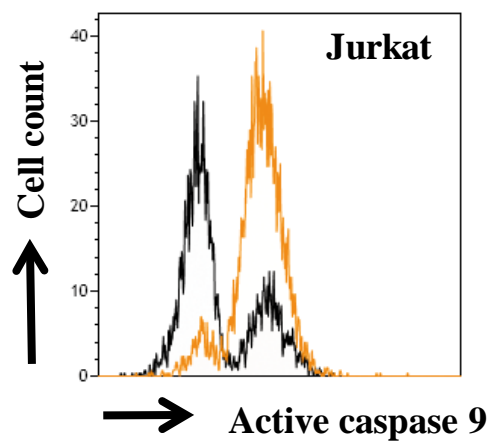
B



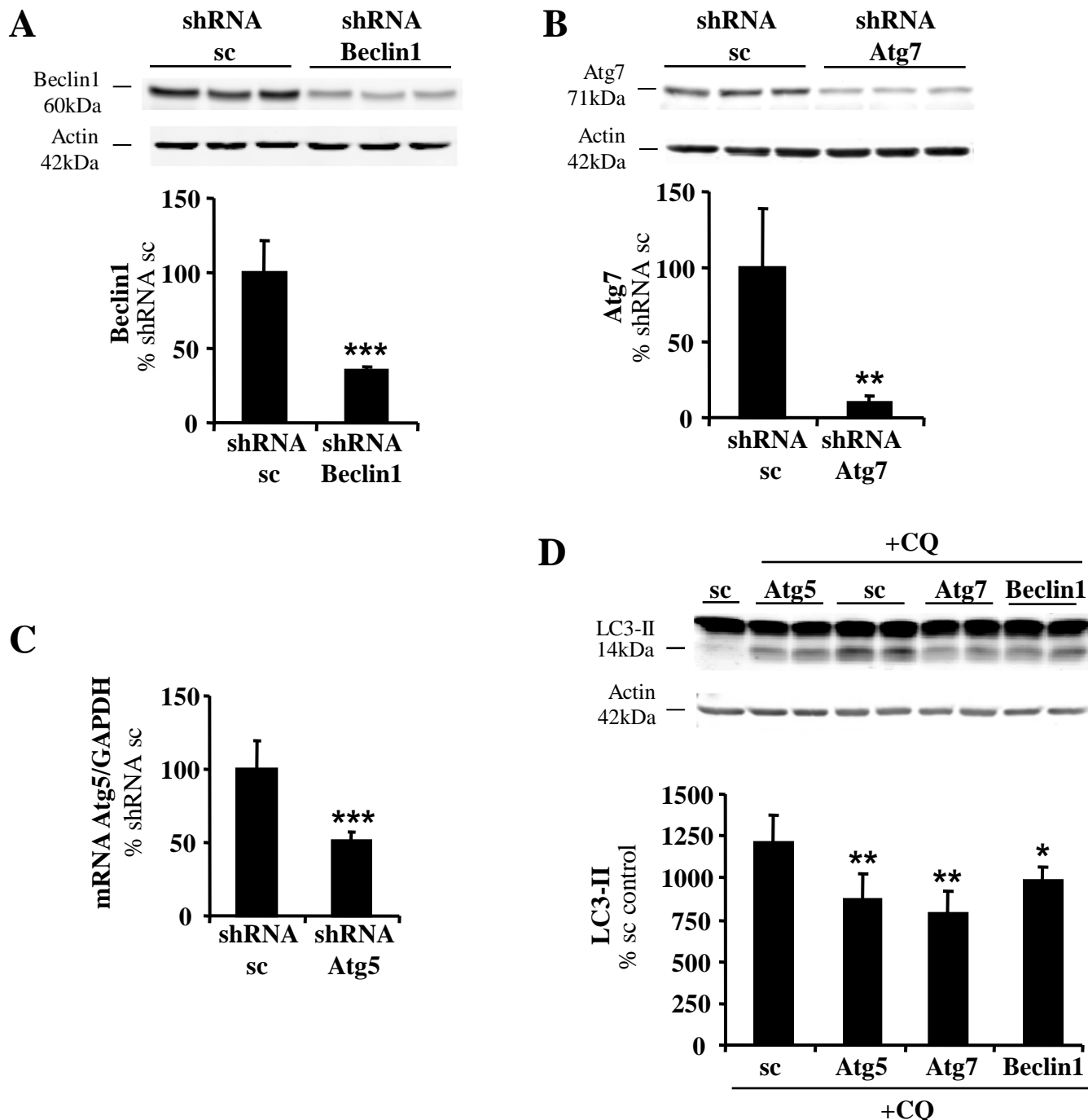
□ Untreated
□ APO866-treated

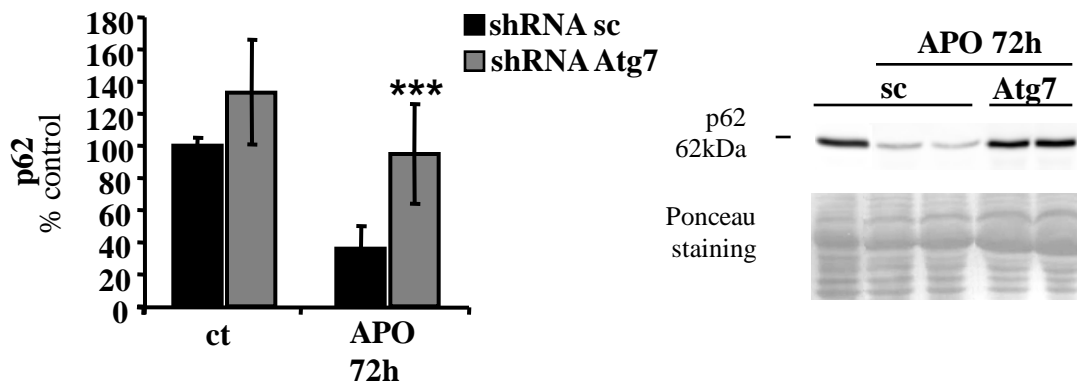
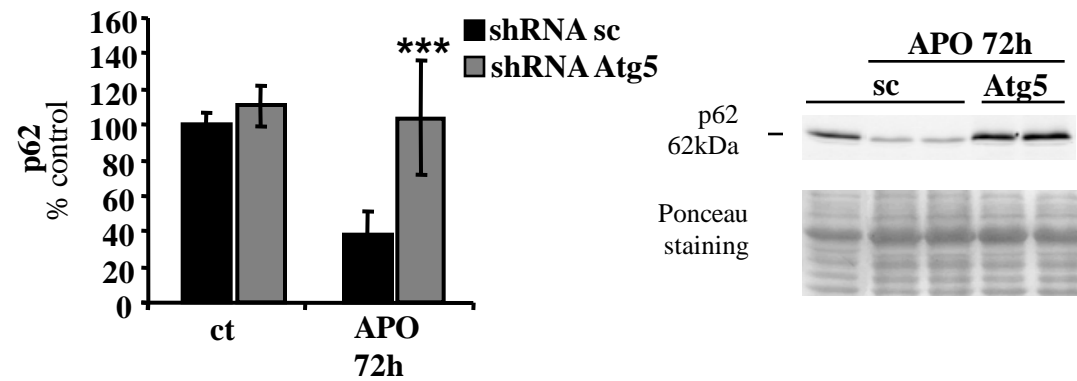
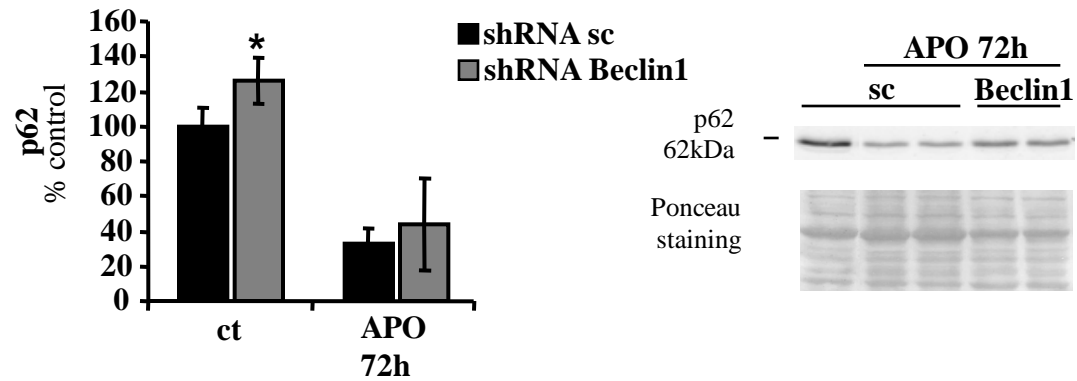


□ Untreated
□ APO866-treated

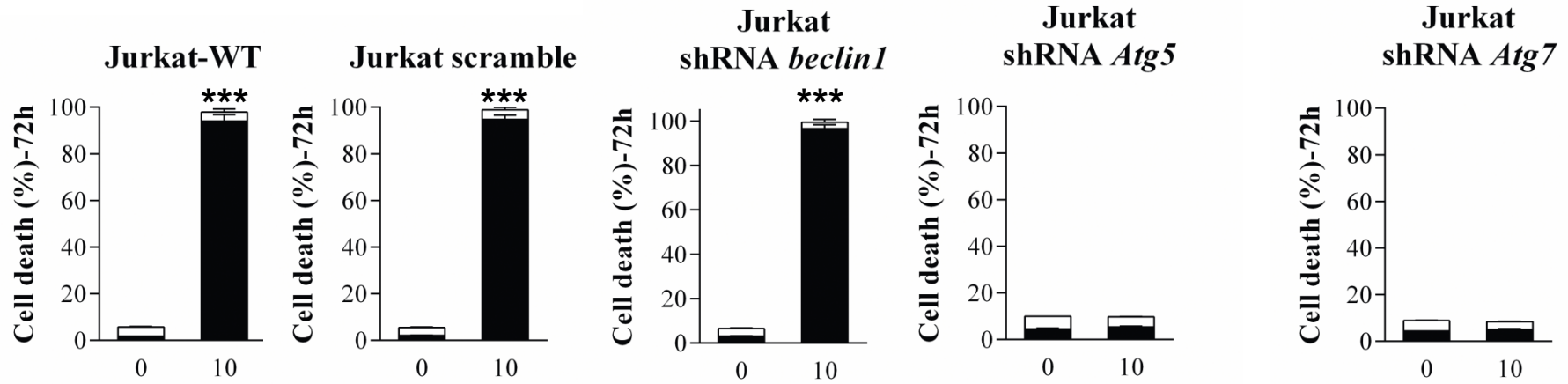


□ Untreated
□ APO866-treated

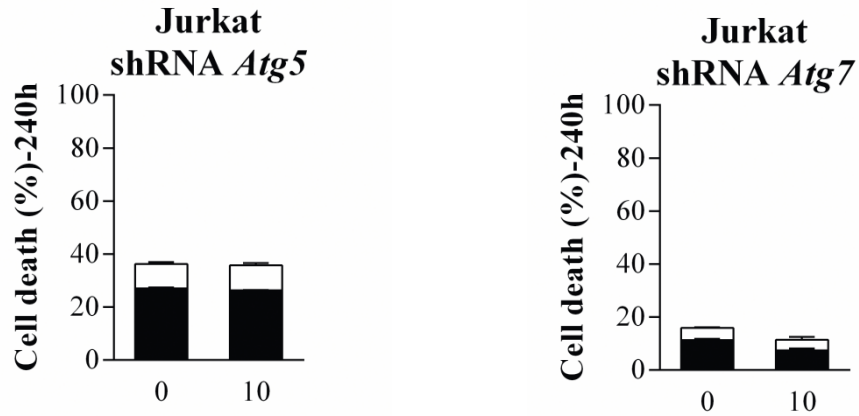


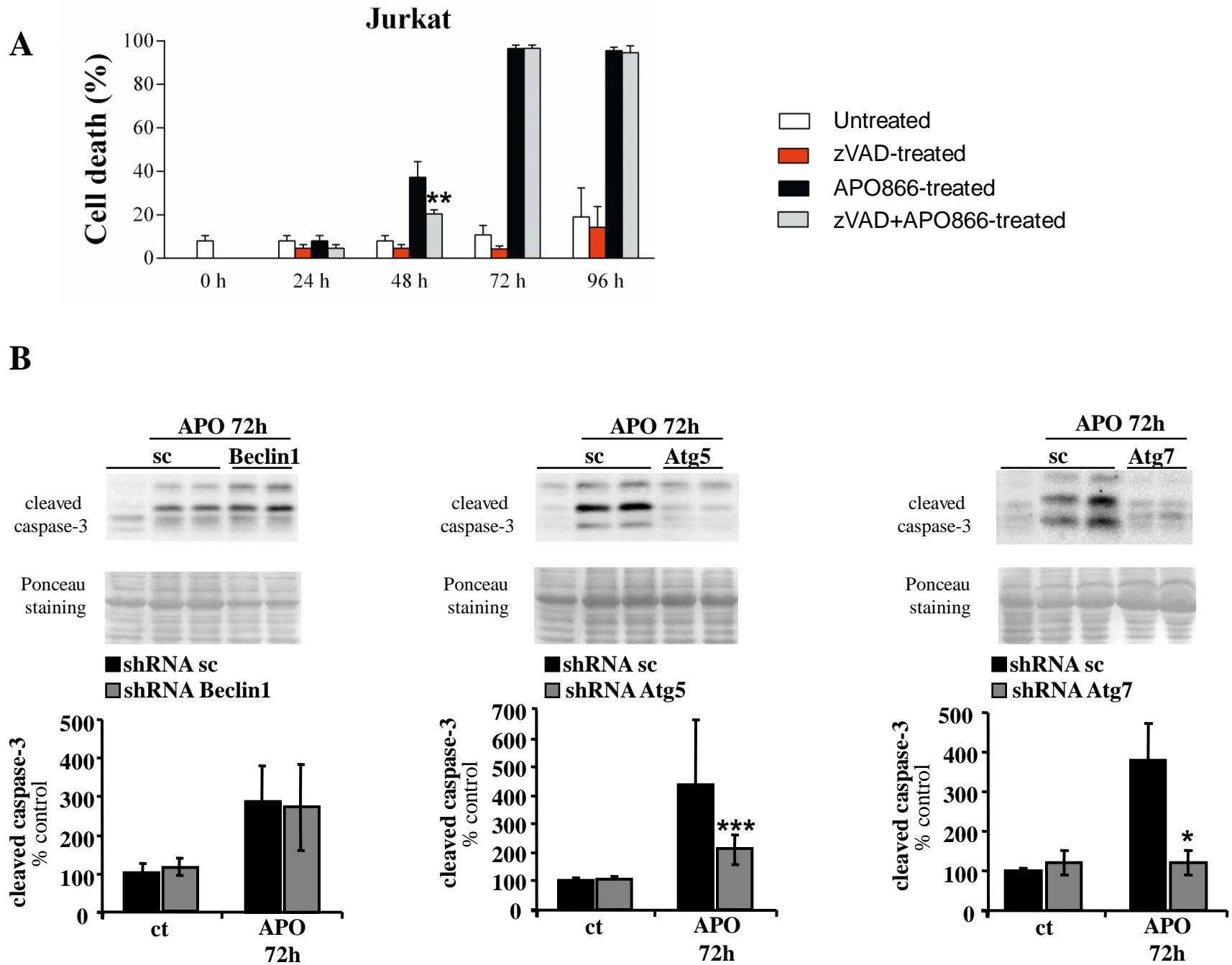


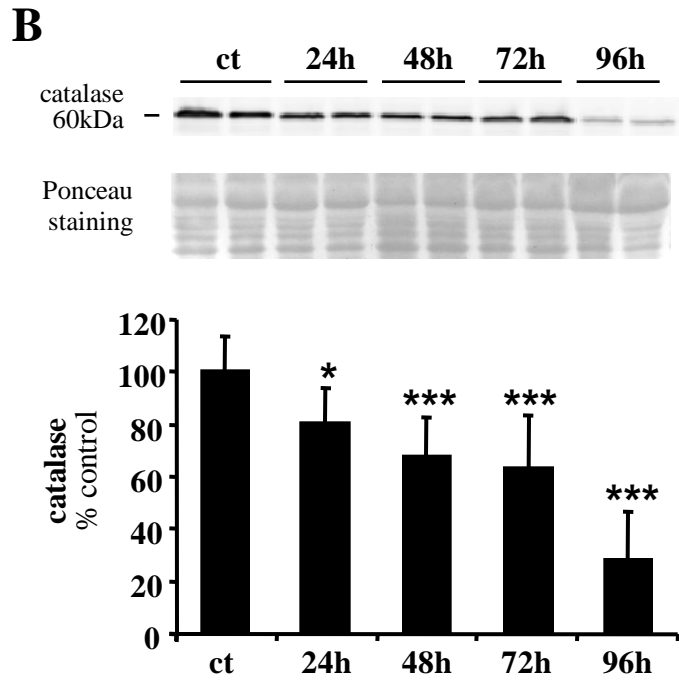
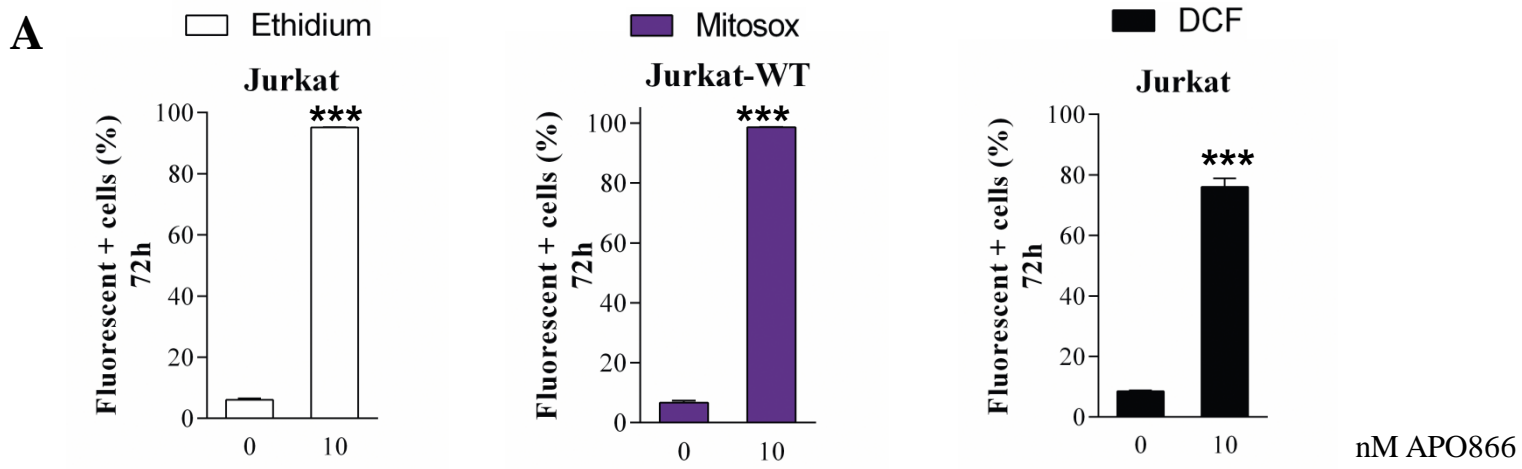
A

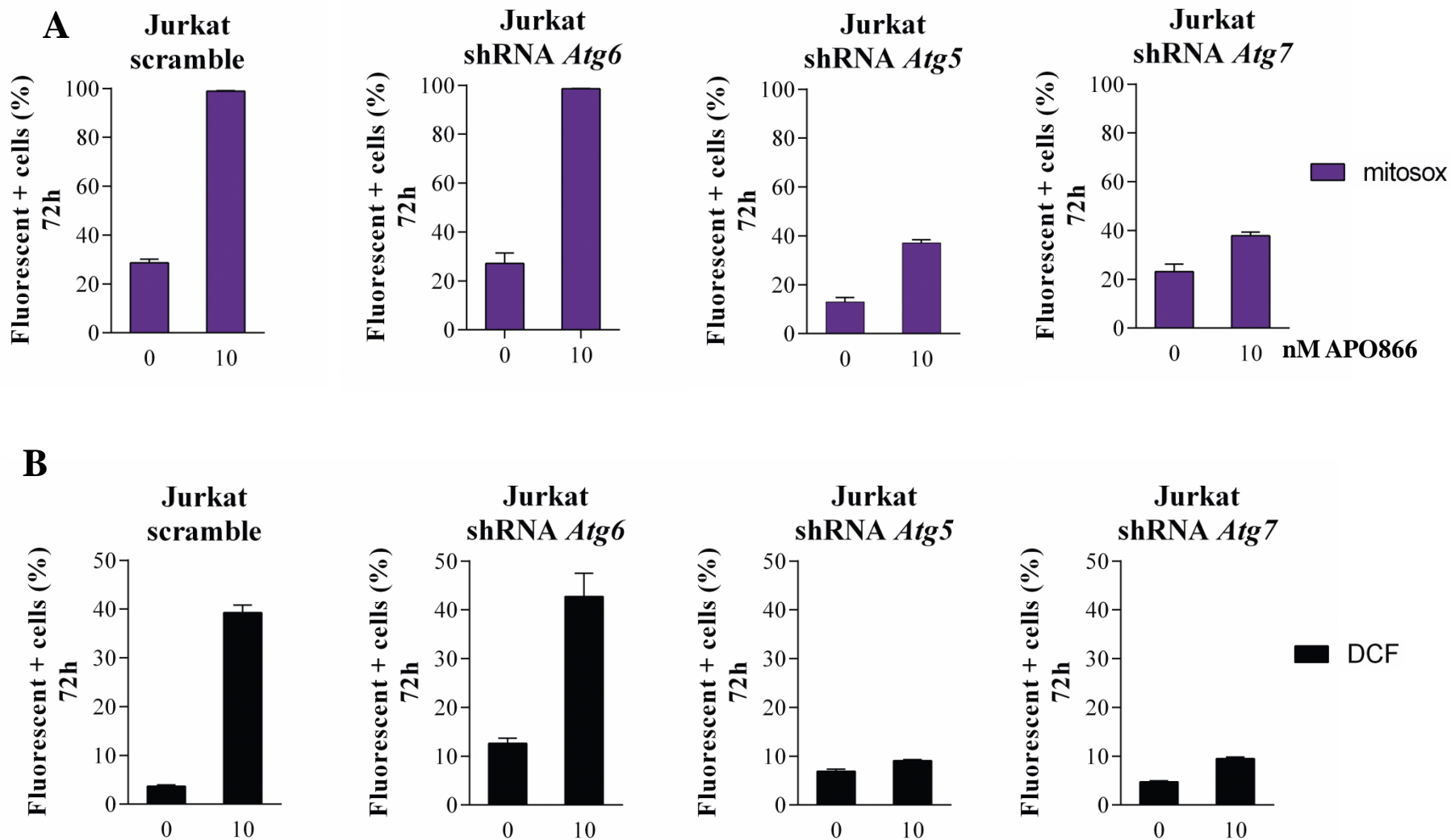


B

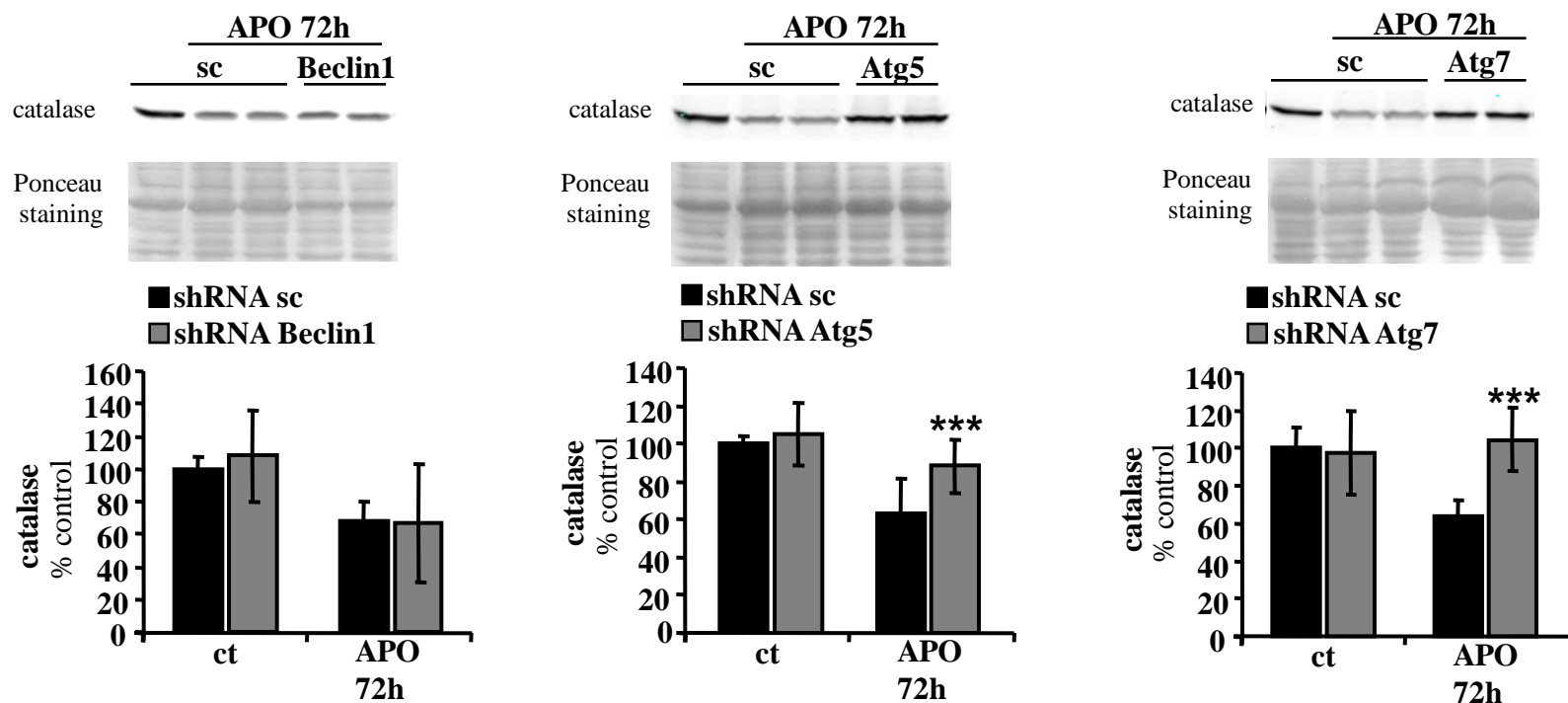




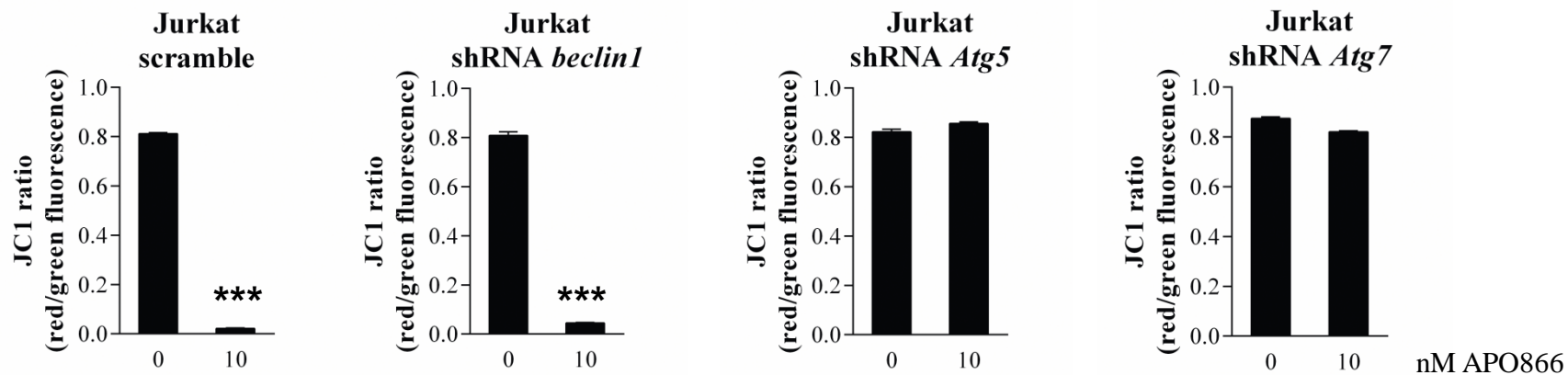




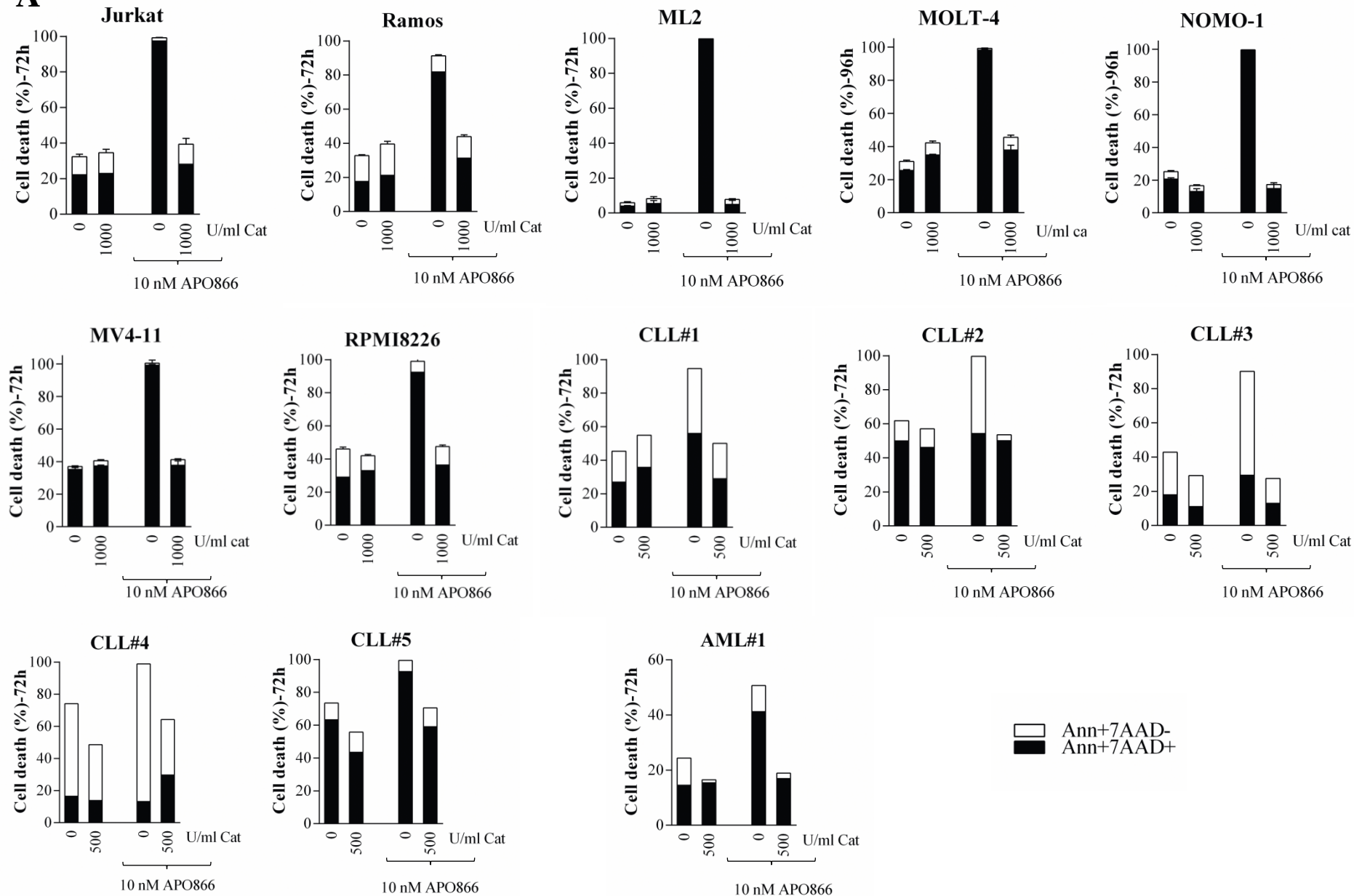
C



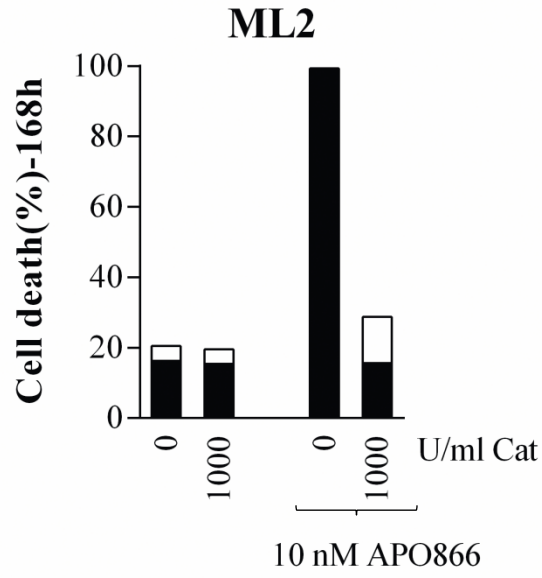
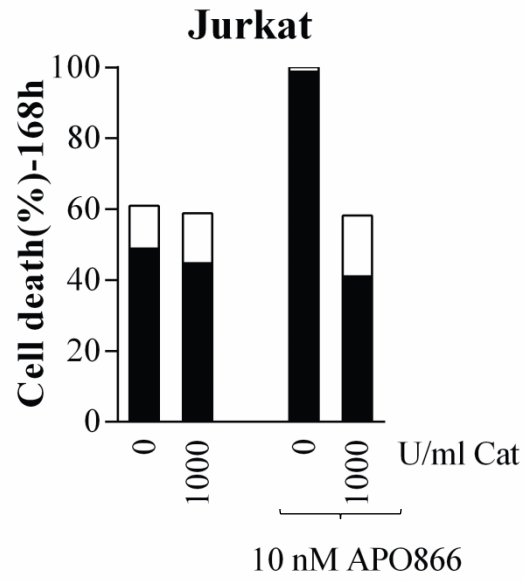
D



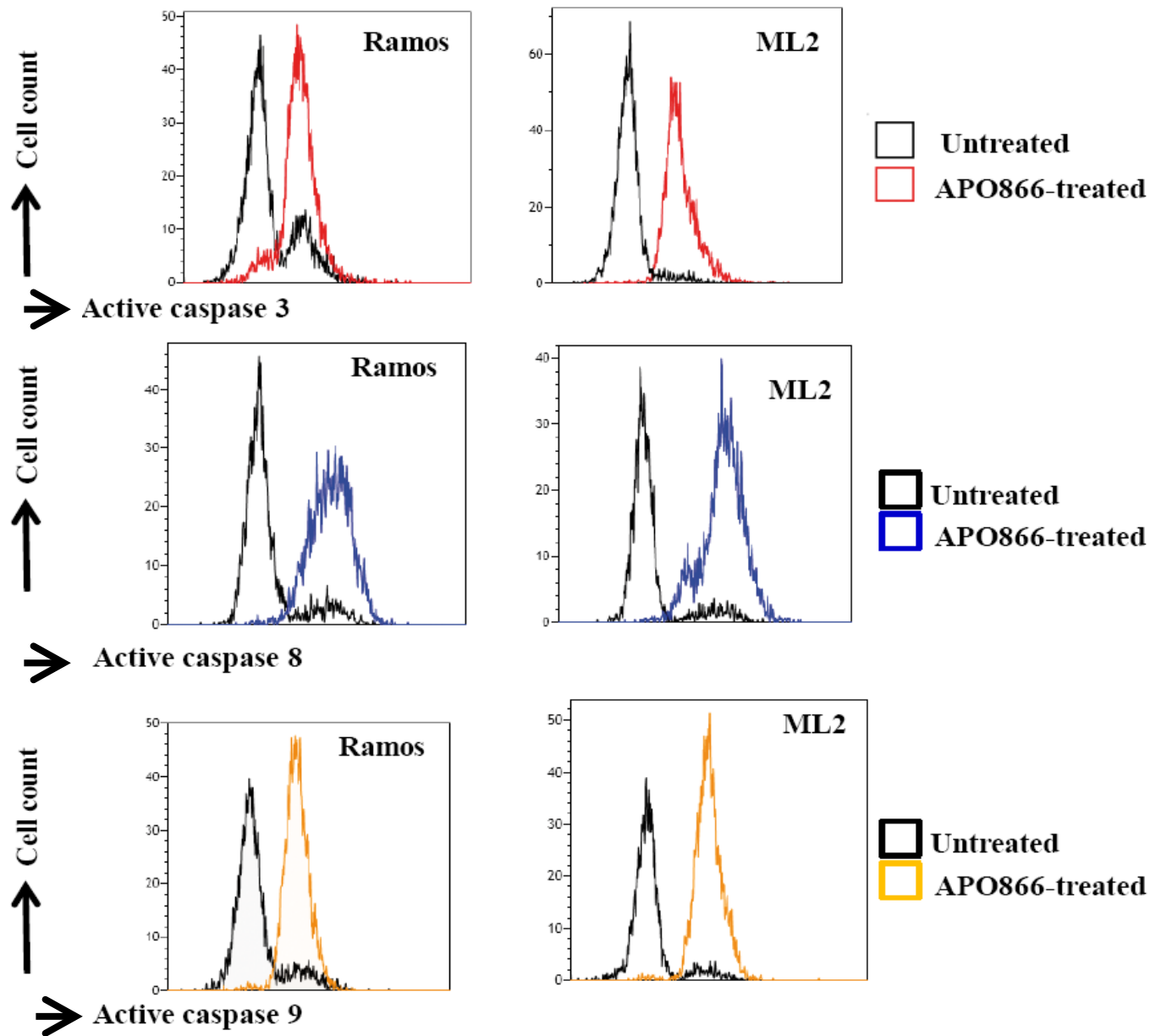
A

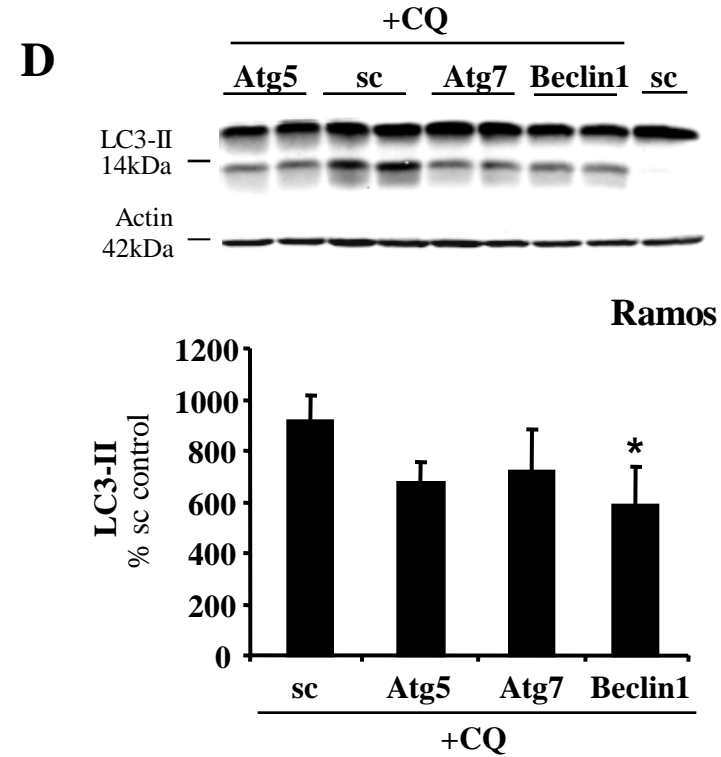
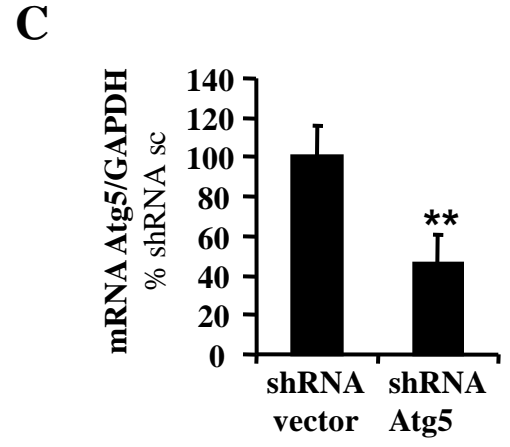
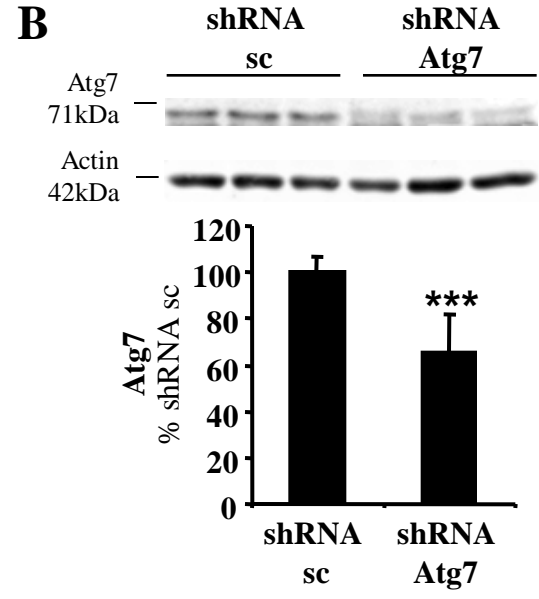
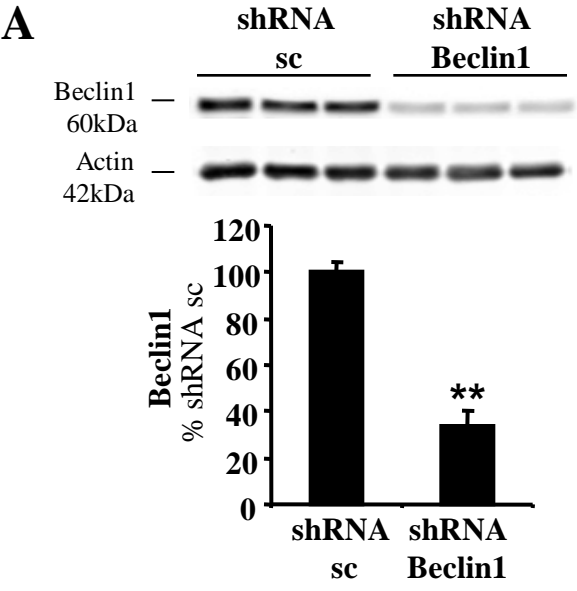


B

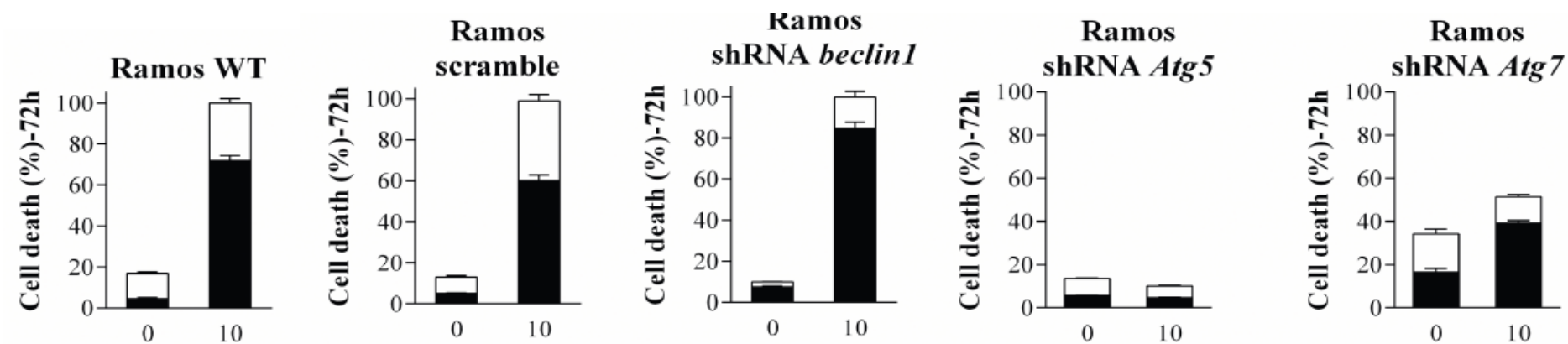


 Ann+7AAD-
 Ann+7AAD+

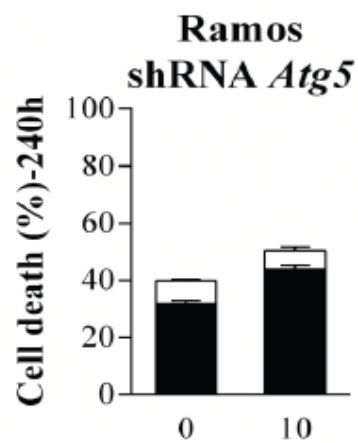
B**Suppl Fig. 1**

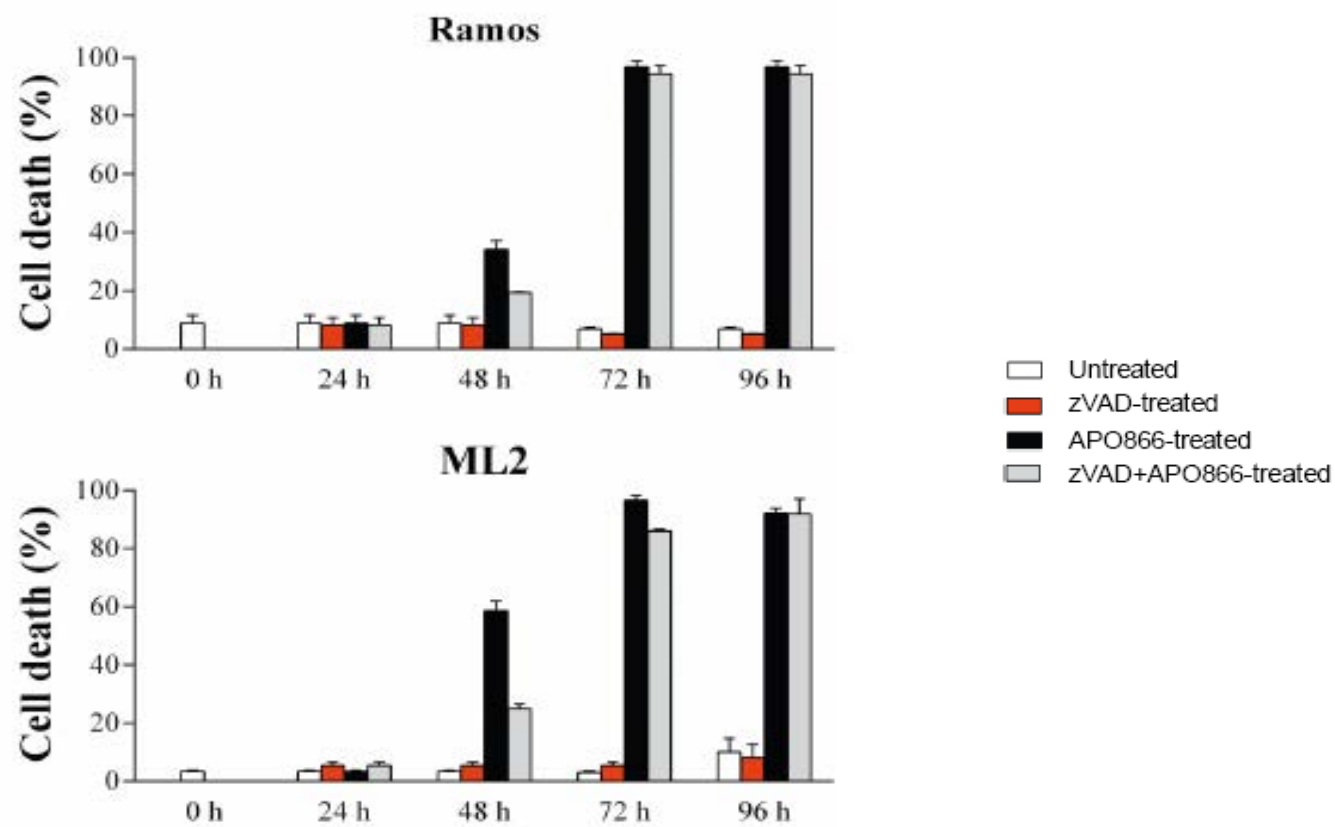


A

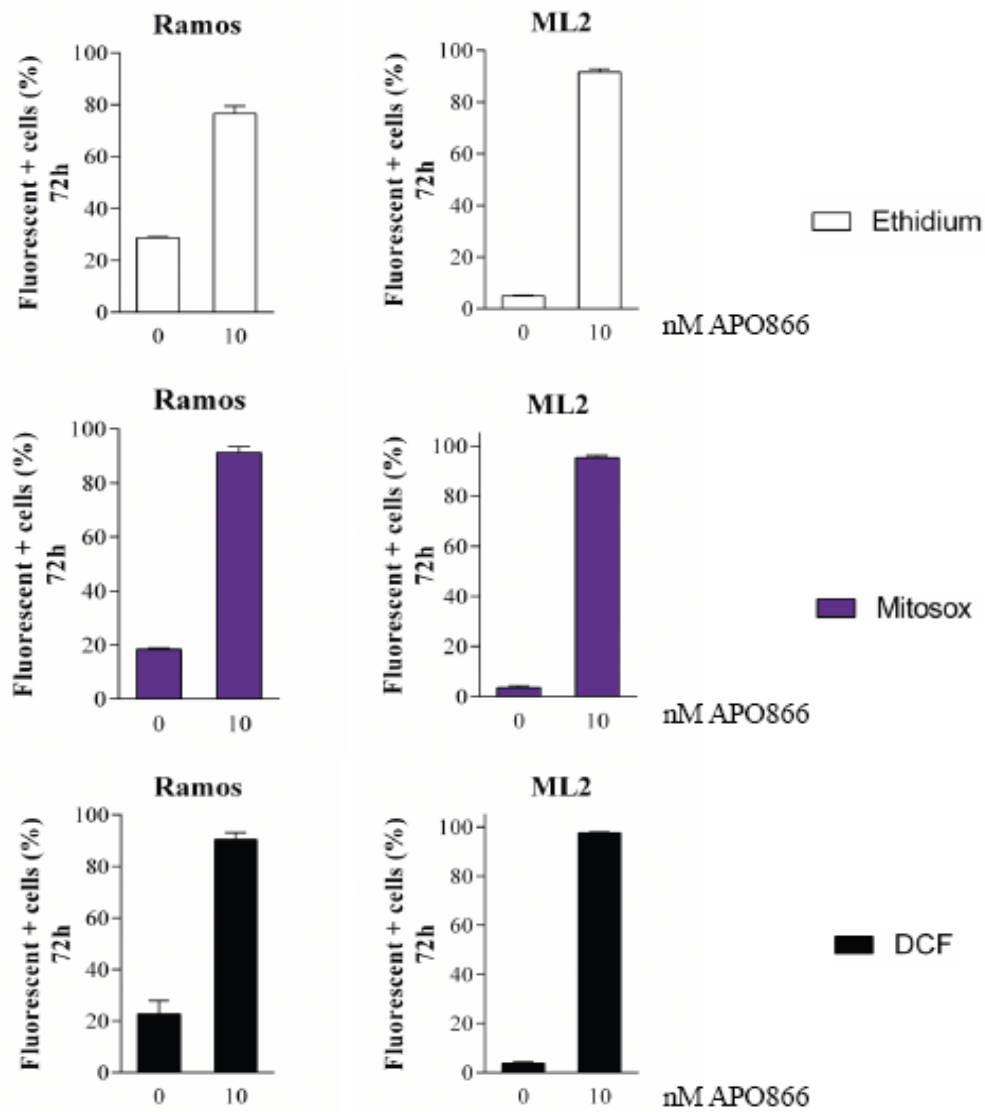


B

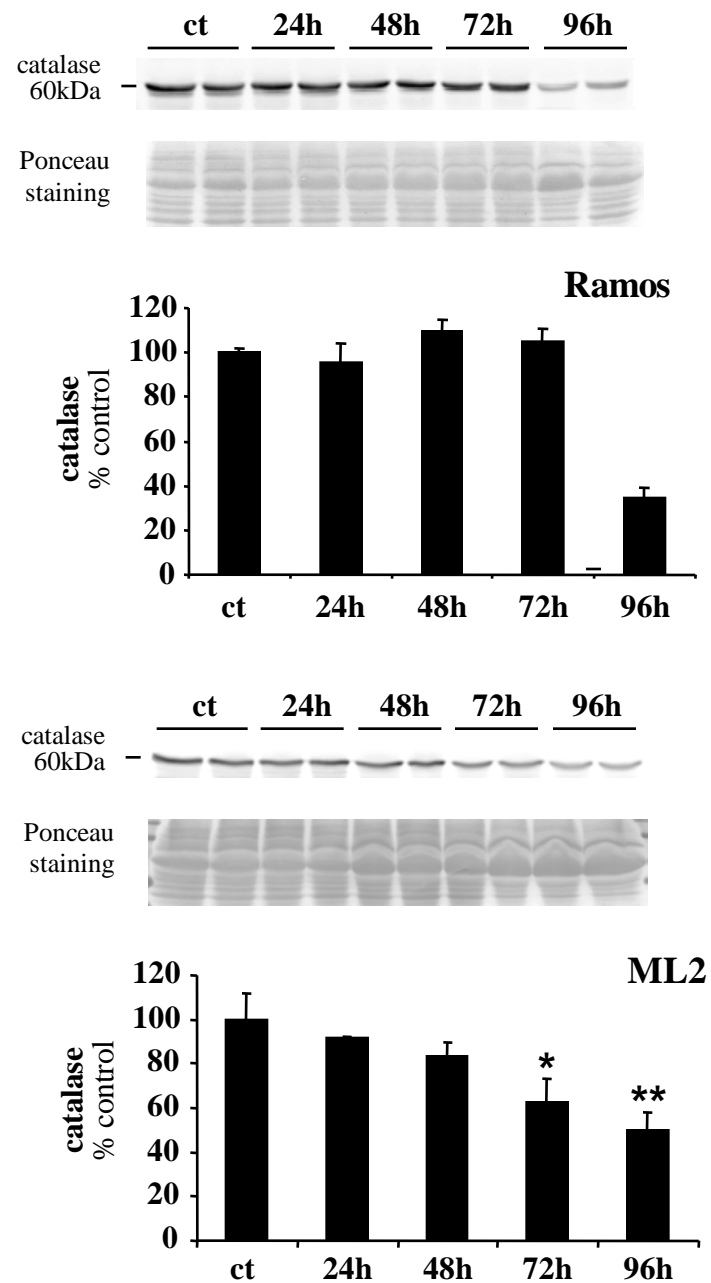




A

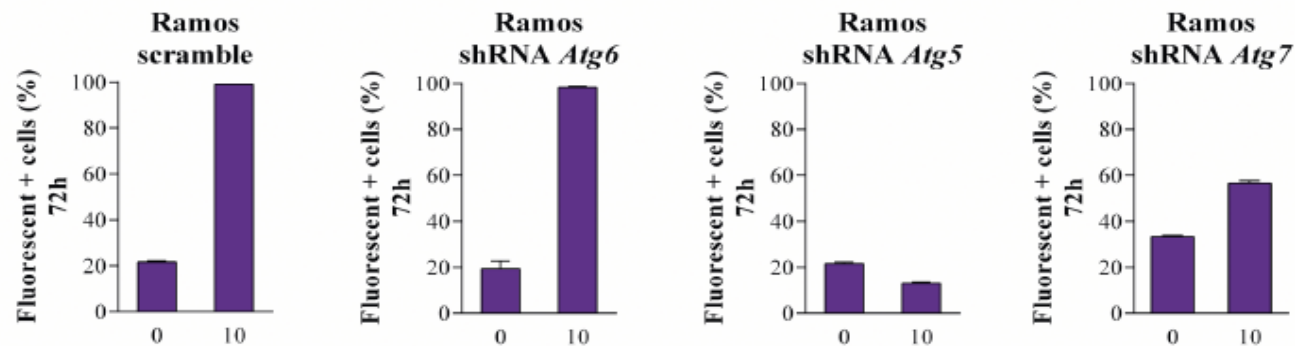


B

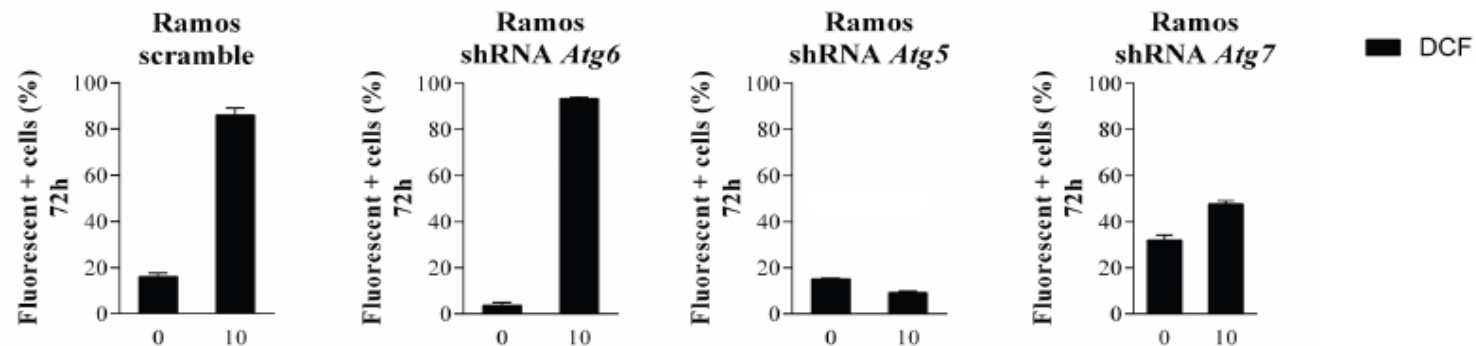


 mitosox

A



B



C

